MODIFIED EUTECTIC ALLOYS FOR HIGH TEMPERATURE SERVICE

By

R. L. Ashbrook
J. F. Wallace

Department of Metallurgy
Case Institute of Technology

INTERIM REPORT

for Contract Period

1 May, 1964 to 1 May, 1965

Grant No. NsG-639

NATIONAL AERONAUTICS AND SPACE ADMINISTRATION

Washington, D. C. 20546

CASE INSTITUTE OF TECHNOLOGY
10900 Euclid Avenue
Cleveland, Ohio 44106

ABSTRACT

27644

The high temperature eutectics Co-10 Al, Co-42 Cr, Co-37 Mo, Co-45 W, Ni-37 Ta, Ni-45 W, and Ni-16 Zr were modified by small additions of Mg, Ca, Y, Ce, La, Ti, Zr, B, Al and C. Unmodified and modified melts were vacuum melted and solidified at three cooling rates and as investment cast test bars. On the basis of microstructure, nine compositions were chosen for mechanical property determination.

The results of stress rupture tests in air at 1800°F as well as room temperature tensile tests of four different high temperature eutectics showed modification capable of producing substantial improvements in properties. Small additions of B, C, and Ti increased the stress rupture lives of the Co-10 Al, Ni-37 Ta, Co-45 W and Ni-45 W up to 23 times and increased room temperature ductility from less than 1 percent to as high as 7.5 percent.

The microstructures were altered in several significant ways to provide these improved properties.

1. Stress rupture life was increased by the formation of carbides or borides in the grain boundaries.
2. Room temperature and high temperature strength were improved by dispersing a subordinate phase more uniformly throughout the matrix.
3. Replacing large continuous or plate-like constituents with small equiaxed or discontinuous phases improved the ductility.

Author

INTRODUCTION

The term "modification" is most familiar in the context of the aluminum-silicon eutectic system (1).* It is used to describe the change in microstructure of the aluminum-silicon eutectic alloys that occurs when they are rapidly cooled from the melt or slowly cooled after being treated with small amounts of sodium. If an aluminum alloy containing approximately 12 percent silicon is slowly cooled from the melt, the resulting microstructure consists of arrays of crudely lamellar silicon plates in a matrix of aluminum solid solution. If the same melt were chill cast, or sand cast after a small sodium addition, the microstructure after solidification would be profoundly "modified". The silicon would then appear in the aluminum matrix as fine, more or less rounded particles.

Recently "modification" has also been used to describe the change from flake to nodular graphite in cast iron, a near-eutectic iron-carbon-silicon alloy (2). The change to nodular or spheroidal graphite is brought about by small additions of cerium or magnesium to a melt that would otherwise develop flakes of graphite on freezing (3).

Chadwick has suggested a general definition of modification to include the effect of small quantities of impurity

- - - - - - - - - -

* Numbers in parentheses refer to the Bibliography at the end of the dissertation.

elements on the microstructures of all eutectic alloys, whether or not there is an accompanying favorable change in the mechanical properties of the alloys (4). Tiller (5) has discussed modification, in the absence of a third phase, in terms of the effect of differences in the solid-liquid interface temperatures of adjacent lamellae on the transition of a lamellar eutectic to a particulate one.

While it may be more proper to limit the term "modification" to those structures that do not contain a third phase, third phases were formed in a number of the compositions studied in the present work. In fact, in some instances one of the binary eutectic phases was completely supplanted by the "third phase". Therefore, for this paper, modification will be defined as "the change in microstructure after solidification of a eutectic alloy brought about by the addition of one or more solute elements or by a change in cooling rate.

It is now realized that modification of eutectic alloys is a general phenomenon which should be applicable to controlling the structure of eutectic alloys melting at high temperatures as well as the structure of the more familiar aluminum-silicon alloy. A number of systems have been shown to be capable of modification, for example, iron-graphite has been modified by magnesium (3); lead-tin by copper (5); aluminum-copper by sodium (6); aluminum-manganese by sodium (6); and lead-antimony by aluminum (6).

Most of the study of the mechanisms of modification of eutectic alloys has centered on the aluminum-silicon system. The mechanism of modification, as of any solidification phenomenon, must be considered primarily in terms of nucleation and growth. Although both nucleation and growth mechanisms are required to explain all the phenomena observed in connection with the solidification of modified aluminum-silicon eutectics, there has been a tendency for investigators to favor one or the other mechanism.

In order to consider the mechanisms of modification let us review some of the phenomena that have been observed during the solidification of aluminum-silicon eutectic alloys.

1. Rapid cooling from the melt produces a modified structure (7).
2. Small ($< .05\%$) additions of sodium and additions of other elements (e.g., calcium, potassium, antimony, boron, titanium, arsenic, etc. (8)) produce modification in sand castings or metal slowly cooled from the melt.
3. In the presence of phosphorus, the eutectic alloy cannot be modified by rapid cooling (7).
4. Phosphorus-bearing melts can be modified but require larger additions of sodium than do melts that are phosphorus free (7).
5. Modified alloys undercool before freezing, yet melt at the equilibrium eutectic temperature (1).

6. The growth of the globular constituent in modified alloys occurs at the same temperature regardless of whether modification is effected by chill casting or by the addition of sodium (9).
7. The greater the silicon content the greater is the amount of sodium required to effect modification (10).

The achieving of a fine particulate distribution of silicon on rapid cooling of the melt is the result of increased supercooling and rapid solidification without permitting diffusion of the silicon atoms over long distances (8). The prevention of undercooling by phosphorus suggests the presence of nuclei, possibly AlP (11) that cause nucleation of silicon to occur at the normal eutectic temperature. This, coupled with the requirement of additional sodium to modify phosphorus-bearing melts, points to a restricted nucleation mechanism. Sodium either is adsorbed on the nuclei (12)(13) or reacts chemically to destroy them (14) (15). Undercooling prior to the formation of a modified structure could occur either because no nuclei were available to start the growth of silicon or because growth was being inhibited by an adsorbed layer of sodium on silicon particles restricting transfer of silicon atoms across the melt-particle interface (4). The fact that modified alloys melt at the equilibrium eutectic temperature (1) invalidates a suggestion (16) that the depressed freezing temperature of modified alloys was the equilibrium freezing temperature of a sodium-

aluminum-silicon ternary eutectic. The solidification of the chill-cast and sodium-modified eutectics at the same temperature is considered (9) as evidence that sodium does not directly affect the growth of silicon. On the other hand, the need for increased modifying additions with increasing amounts of silicon (10) suggests a relation to the amount of silicon surface area on which sodium might be adsorbed.

Despite the relatively great attention the modification of the aluminum-silicon eutectic has received, there is no general agreement on why modification takes place. Probably both restricted growth and restricted nucleation, as well as other mechanisms, operate in the modification of the aluminum-silicon eutectic and other eutectic systems.

It has been shown that modification of a binary eutectic can be effected by addition of a solute element that has greatly different distribution coefficients or k values in the two phases of the eutectic. Under these conditions, differences in the temperatures at the solid-liquid interfaces of the two phases retard the growth of one phase with respect to the other (5). It has also been shown that a transition from a rod-like eutectic to a globular eutectic would be expected with increasing undercooling (17). A mechanism applicable to the transition from lamellar to rod-like eutectics depends on the concept of constitutional supercooling (18). With increasing supercooling the leading lamellae would bridge over the lagging phase at

intervals along their length so that the growth of the exposed surfaces of the lagging phase could only continue in a rod-like fashion. With further supercooling, the leading phase would grow completely over the second phase so that the growth of the second phase could continue only after renucleation at or near the solid-melt interface. Repeated nucleation would result in a particulate distribution of the subordinate phase.

A comparison of the particulate silicon phase in a sodium modified aluminum-silicon eutectic and of the plate-like silicon phase of an unmodified aluminum-silicon eutectic is made in Figure 1 (19). The alloy shown is the hypoeutectic aluminum alloy A356 which has the composition Al - 7.0 Si - 0.3 Mg. The dark plates of silicon exhibit a coarse, somewhat lamellar, pattern in the unmodified alloy, while in the sodium modified alloy, silicon is present as small more or less rounded particles. The large white areas in the micrographs of both conditions are sections through primary aluminum dendrites.

The effect of sodium modification on the tensile properties of A356 as a function of distance from a chill can be seen in Figure 2 (19). Generally, the ultimate tensile strength and percent elongation were substantially increased and the yield strength slightly increased with increasing distances from the chill. However, at short distances from the chill, the tensile strength and ductility were depressed by modification. Although

the authors offered no explanation for the poorer properties in the vicinity of the chill, this condition may have been the result of overmodification (20). It has been shown that maximum properties are not achieved at maximum sodium content, and that in chill castings of Aluminum-13 silicon alloys, maximum ductility is achieved at lower sodium content than for sand castings (21). The beneficial effects of modification on strength and ductility are more pronounced in higher silicon content alloys, for example, modification of a sand cast 13 percent silicon alloy raised the average tensile strength from 18,000 psi to 25,000 psi and the elongation from 2 percent to 13 percent (2).

Although this discussion has thus far been limited to room temperature properties, eutectic alloys should also be of interest for high temperature service. Although "high temperature eutectic alloys" may appear to be a contradiction in terms, many eutectic systems including those studied in this program have melting points in excess of 2400°F. One of the mechanisms by which high temperature alloys are strengthened is dispersion of a relatively brittle phase such as an oxide, carbide, or an intermetallic compound throughout a ductile matrix. In general, strength is increased by decreasing the size and spacing of the dispersed particles (22) (23). Furthermore, room temperature ductility may also be increased by changing the shape of a brittle dispersed phase from plate-like

to equiaxed or spheroidal (8).

When a dispersion-strengthened alloy is obtained by precipitating a non-coherent dispersoid from a solid solution, it must be possible to take the hardening phase into solution in order to distribute it by subsequent aging treatments. Because of this, overaging and resolutioning limit the maximum temperature to which such alloys can be used. However, in a binary eutectic system, both phases coexist up to the melting point. This suggests that a stable dispersion hardened cast alloy would result if a sufficiently fine distribution of one of the eutectic phases could be obtained during solidification.

An additional reason for interest in eutectic alloys is their excellent castability. Many problems arise in making castings from alloys with a wide spread between the liquidus and solidus temperature. The smaller the spread, the better the casting behavior (24). A narrow liquidus to solidus spread provides: (1) improved fluidity, (2) longer feeding distances, and (3) a reduced tendency to hot tear. Since eutectic alloys, like pure metals, freeze at a single temperature rather than over a range of temperatures, they are far better as casting alloys than a solid solution alloy with a long liquidus to solidus range.

The purpose of this research was to study the effects of small solute additions on the microstructure and mechanical properties of a number of high melting point eutectic composi-

tions. The aim was two-fold: (1) to obtain a better understanding of the modification of eutectic alloys and (2) to develop a new means for improving the properties of high temperature alloys by controlling structure. Although it has been reported that the optimum high temperature properties in eutectic systems do not occur at the eutectic composition (25), it appeared desirable as a first step in exploring the modification of high temperature eutectic systems to limit this investigation to alloys of eutectic composition. When the structures of eutectic compositions can be effectively controlled, it should be possible to extend this control to hypo- or hyper- eutectic compositions where eutectic structures can also be influenced by modification.

EXPERIMENTAL PROCEDURE

ALLOYS INVESTIGATED

Seven binary eutectics having melting points greater than 2400°F were chosen for investigation. They are shown below with their melting points and the phases which form the eutectics (26).

Second Element	Weight Percent of 2nd Element	Eutectic Phases	Melting Point
Cobalt-base			
Al	10	Co-CoAl	2552°F
Cr	42	Co-δ	2552°F
Mo	37	Co-Mo_6Co_7	2444°F
W	45	Co-W_6Co_7	2696°F
Nickel-base			
Ta	37	Ni-Ni_3Ta	2480°F
W	45	Ni-W	2732°F
Zr	16	Ni-$ZrNi_4$	2516°F

Potential modifying elements were chosen from Groups II, III, and IV of the periodic table. They met one or more of the following requirements:

1. They were chemically reactive.
2. They met the criteria of:
   a. greatly differing k values in the two phases,
   b. greatly differing liquidus slopes for the third element.

3. They had been shown to be effective modifiers in other systems (3) (8).

4. They had been shown to be effective grain refiners in other systems (27) (28).

The additions used all came from Groups II, III or IV and are listed below:

Group II a	Group III a	Group IV a	Group III b	Group IV b
Mg	Y	Ti	B	C
Ca	La	Zr	Al	
	Ce			

Generally single additions of 0.1 percent of the weight of the melts were made. However, some additions as large as 1.0 percent by weight were used as well as complex additions containing up to four elements. A complete list of the additions made to the several eutectic systems is shown in Table I.

On the basis of microstructure the nine modified eutectic alloys listed below were chosen for further evaluation.

Co-10 Al + 1.0 C
Co-45 W + 0.2 C
Ni-37 Ta + 1.0 C
Ni-45 W + 0.1 B
Ni-45 W + 0.1 C
Ni-45 W + 0.1 La
Ni-45 W + 1.0 Ti
Ni-45 W + 0.1 Y
Ni-45 W + 0.1 each B, C, Ti, Zr

These modifications as well as the corresponding unmodified alloys were cast as test bars for stress rupture and tensile testing.

MELTING AND CASTING MATERIALS AND TECHNIQUE

The melting stock was high purity material of the form and purity listed:

Element	Form	Purity
Aluminum	granulated ingot	99.9 +
Boron	-325 mesh	99.25
Carbon	spectroscopic graphite	99.999 +
Calcium	turnings	98.0
Cerium	cast ingots	99.9
Cobalt	electrolytic 1" x 1" x 1/8"	99.5 +
Chromium	electrolytic	99.8 +
Lanthanum	cast ingot	99.9 +
Magnesium	turnings	99.4
Molybdenum	powder, 4 microns avg.	99.0
Nickel	electrolytic 1" x 1" x 1/8"	99.9 +
Tantalum	roundels	99.5
Titanium	sponge	99.65
Tungsten	powder, 6 microns avg.	99.9 +
Yttrium	turnings	99.9
Zirconium	sponge (reactor grade)	99.8 +

Chemical analyses were obtained from an independent laboratory for test bar melts representing thirteen compositions that were tested for mechanical properties and for six of the exploratory melts.

The molds for the melts used to study microstructures combined a pouring cup and a cylindrical section, made from calcium aluminate bonded fused silica, with a copper chill mold. The cylindrical mold section had a cavity 3/4" diameter by 2" long. The cavity in the chill mold was 5/8" in diameter by 1/2" deep. The sections of the mold are shown in Figure 3, an assembled mold in Figure 4, and a typical casting from the composite mold in Figure 5. Ceramic shell molds with a dip coat refractory of zircon and made by the lost wax process were used for casting test bars. Dewaxed shell molds backed with unbonded grog (burned fire clay) were maintained at 1600°F in the vacuum chamber by a small resistance furnace. Figure 6 shows a shell mold and a cluster of test bars cast in a similar mold.

Vacuum induction melts for microstructure determination were made at Case Institute of Technology. Test bars were vacuum cast at Lewis Research Center. The Case furnace was powered by a 960 cps motor-generator. The NASA furnace was powered by a 9,600 cps motor generator. In both installations melting was done in zirconia crucibles surrounded by graphite susceptors.

For exploratory melts an assembled composite mold was placed in the vacuum chamber, and a crucible containing the complete 60 cc charge (except for large carbon or volatile additions) was inserted in the susceptor. The chamber was pumped to a pressure of 5 microns mercury before power to the

induction coil was turned on. After 15 minutes, melting had usually begun. When carbon additions were made it was sometimes necessary to introduce argon to suppress a carbon boil. Volatile additions such as magnesium or calcium were made under a pressure (always less than atmospheric) of argon. After melting was complete the temperature was increased to assure the solution of the high melting point element. The melt was then cooled until solidification occurred. The freezing temperature, read by means of an optical pyrometer was used as a reference point for establishing the pouring temperature which was at a reading of 200°F above the melting point. The actual superheat was approximately 340°F. When the casting was poured, a portion of the melt approximately 3/4 inch deep was retained in the crucible. This was permitted to solidify under reduced power to obtain a sample solidified at a relatively slow rate.

The melting procedure for the test bar castings was essentially the same as that used at Case. However, the size of the melt, which was approximately 170 cc, necessitated the addition of metal during melting. The complete charge, except for about 30 percent of the nickel or cobalt, was placed in a new crucible. The extra metal was loaded into an additions maker. The crucible was inserted in the induction coil, and a preheated mold was put into the mold heating furnace at 1600°F. The vacuum chamber was pumped to pressure less than 5 microns

mercury before power was turned on. After all the nickel or cobalt had been added to a tungsten bearing melt it was superheated, 350°F (optical) to dissolve tungsten. With power off, the melt was then permitted to freeze to obtain a reference temperature for casting. A 200°F (optical) superheat was used for casting. Measured optically through a mirror and a 1/4" thick pyrex sight glass, 100°F was equivalent to approximately 170°F actual, as measured with a tungsten vs. tungsten-rhenium thermocouple.

It was found that the holding times and temperature that had been adequate to dissolve tungsten powder in the 960 cycle furnace with its vigorous inductive stirring left a tungsten residue in the crucible in the 9,600 cycle furnace which stirred the melt only slightly. To correct this condition the times and temperatures were increased.

The molds were left in the vacuum chamber for 15 minutes after casting and then allowed to cool to ambient temperature in air prior to removing the mold material from the casting. After cut-off the test bars were visually inspected with the aid of fluorescent penetrant.

METALLOGRAPHIC WORK AND MECHANICAL PROPERTY DETERMINATIONS

Three portions of each melt, representing three different cooling rates, as well as sections cut from test bars were examined metallographically. Cobalt-base alloys were etched electrolytically in a solution made of 6 parts sulfuric acid,

30 parts saturated solution of boric acid and 30 parts of water. Stains were removed with ammonium hydroxide. Nickel-tungsten and nickel-zirconium alloys were etched electrolytically with 10% oxalic acid in water and the nickel-tantalum alloys were swabbed with a solution of 30 parts acetic acid, 5 parts nitric acid and 5 parts hydrofluoric acid. The phases observed were not identified by means other than metallography. It was assumed that the phases that combined to form the unmodified binary eutectic structures were those defined by Hansen (26). The microconstituents of some of the third phases had been described in the literature or were observed in binary alloys prepared during this research.

Stress rupture testing was done with as-cast (unheat-treated, cast to size) test bars. The test bars which were shown in Figure 6 were from a design used by NASA (29). The gauge section was 1-1/4 inches long and 0.250 inch in diameter. All stress rupture tests were performed in air at 1800°F. Room temperature tensile tests were also performed with unheat-treated and unmachined bars. An exception was made for a few compositions where the first bar tested was very brittle or showed evidence of intergranular oxidation. Under these circumstances, subsequent bars were ground to improve their surface or to remove the skin containing the intergranular oxidation.

RESULTS AND DISCUSSION

CHEMICAL ANALYSIS

The chemical analyses of test bars representing alloys tested for mechanical properties and of six exploratory heats are listed in Table II. The average recovery of tungsten in exploratory melts that were analyzed was 44.2 percent, for a 45 percent addition. For test bar melts the recovery averaged only 41.76 percent not including melt No. 242 which was reported separately. Melt No. 242 which was one of the first test bar melts made had a tungsten content of only 37 percent. The residue of tungsten found in the bottom of the crucible after pouring this melt was attributed to the reduced stirring obtained in the 9,600 cps induction furnace. The lack of stirring resulting from the high frequency power supply was compounded by the necessity of using a susceptor to avoid cracking the crucible by thermal shock. Increasing the holding times and temperature raised the recovery to nearly 44 percent for some melts, but resulted in a pick-up of zirconium from the crucible. Most of the test bar melts showed a zirconium content greater than 0.01 percent, while a nickel-37 tantalum plus 1.0 carbon melt heated to approximately 3700°F contained 0.55 percent zirconium.

Recovery of the other additions varied considerably depending on the amount added and their reactivity. The recovery of aluminum and tantalum was high. The carbon loss

was approximately 10 percent of that added in most cases; no loss was reported for carbon in the cobalt-10 aluminum melt and a slight increase occurred in the nickel-45 tungsten heat to which the four elements boron, carbon, titanium and zirconium were added. The boron recovery was approximately 50 percent in the exploratory heats but 80 percent or over of this element was recovered in the test bar melts.

Even though the recovery of some elements varied between the melts in the lower (exploratory) and higher (test bar) frequency melting furnaces, the structures were comparable in most cases. A comparison in Figures 7 through 18 of part d, which represents a section from a test bar, with parts a, b and c, which represent sections from the composite mold castings, shows that the structures obtained in both types of casting were substantially the same. Even though the composition of the tungsten-bearing test bars was hypoeutectic, the hypereutectic primary phase was present in the test bars if it was also present in the exploratory casting. The chief difference was that zirconium could be seen in the test bars as a pink phase in dendrite arm boundaries of the matrix but was not present in the exploratory heat. This element was probably responsible for a slight thickening of the tungsten constituent in the structures illustrated.

Two sharp differences in structure did occur. The structure of the 0.1 yttrium modified nickel-45 tungsten test bars

was radically different from that of the corresponding exploratory casting. The lanthanum modification of this same base also showed differences between the structures of the two types of melt. Recovery of both yttrium and lanthanum was low in the test bar melts.

Some evidence exists that primary tungsten phases settle out of the castings by gravity during solidification. Opposite ends of one casting from each of two heats were analyzed for tungsten. The unmodified nickel-45 tungsten alloy in which the tungsten was present, largely as a eutectic constituent, showed relatively little segregation. The nickel-45 tungsten plus one percent titanium in which tungsten was chiefly a primary or proeutectic constituent showed substantial segregation; the top of the test bar contained 34.7 percent tungsten and the bottom 43.8 percent tungsten.

MICROSTRUCTURAL CONSIDERATIONS

A summary of the microstructures of all the exploratory melts made is shown in Table I. The morphologies of the eutectic constituents, the primary phases present and the macrostructures are listed for the ceramic-cast 3/4 inch diameter cylinder. The distribution of the brittle phase, whether continuous or particulate, is shown for the zone near the chill-metal interface. Figures 7 through 19 illustrate the microstructures of seven unmodified binary eutectics as well

as the microstructures of six modified alloys from four of the eutectic systems. These six modified alloys are those whose stress rupture properties were improved by modification. Figures 20 through 25 show the 1800°F stress rupture properties and room temperature tensile properties of the alloys tested. Average mechanical properties are listed in Table III and the complete stress rupture and tensile data are listed in Tables IV and V respectively.

The discussion of microstructures will be centered largely on the structures observed in the 3/4 inch diameter cylinders. Reference will be made to the structures of the chill casting and of the portion of the melt cooled in the crucible only when this sheds additional light on the solidification process. Ten of the figures each contain four photomicrographs: three showing sections representative of the three cooling rates in the exploratory melts, and one showing a section from an investment cast test bar from a melt to which the same additions were made.

Since orientations of the phases were not determined, no exact classification of the eutectic structures as normal, anomalous or degenerate was possible (30). It was also not feasible to classify them as continuous or discontinuous on the basis of a two-dimensional section. Few of the compositions cast were completely "eutectic" in the sense that primary or proeutectic constituents did not occur. In many

instances, dendrites or primary constituents of the phases on both sides of the eutectic were present in close proximity, a condition that has been observed in other systems (31).

Effect of Cooling Rate on Microstructure

Changes in cooling rate can have profound effects on the microstructure of eutectic alloys. As was discussed earlier the aluminum-silicon eutectic can be modified without additions of modifying agents if it is solidified rapidly (8). In the iron-carbon-silicon system one of the constituents of the eutectic can be changed to another species, if the melt is rapidly cooled (32). It has also been pointed out that if the cooling rate is sufficiently rapid, it should be possible to change a lamellar eutectic to a particulate eutectic (5). In recognition of the effect of cooling rate on structure the exploratory melts were solidified at three different rates.

Although the constituent size was generally finer in that part of the casting cooled in the chill mold than in the ceramic mold, it was found that no composition developed a completely particulate eutectic structure in the chill mold that did not also develop such a structure in the ceramic mold. However, in some of the chill castings, a narrow zone on the order of 0.005 to 0.010 inch thick occurred next to the chill where the structure consisted of discrete particles of the subordinate phase in the cobalt or nickel solid solution matrix. Only in this zone can true "modification" be considered to have

occurred. Whether a particulate or continuous second phase was found next to the chill is indicated in the last column in Table I.

A particulate distribution of the subordinate phase in the chilled region invariably resulted from boron-containing additions. However, in the cobalt-base alloys, a continuous brittle interdendritic boron-rich eutectic connected the particles of the subordinate phase of the original binary eutectic. In the nickel-base alloys, boron did not form a continuous embrittling eutectic constituent. In addition to boron, 0.1 titanium carbide produced a particulate eutectic zone in the cobalt-42 chromium chill casting. A particulate distribution was also found in the cobalt-45 tungsten alloys modified by the following additions: 0.2 magnesium, 0.2 calcium, 1.0 titanium, 0.1 boron, 0.1 carbon and 1.0 carbon. All the nickel-37 tantalum alloys other than the 1.0 carbon modification developed a zone at the chill interface consisting of minute plates of $TaNi_3$. In the 1.0 carbon modification equiaxed carbides occurred instead. Except for the unmodified alloy and the alloys modified with 0.1 cerium and 0.1 titanium, all the nickel-45 tungsten chill castings had a particulate zone in which tungsten or, in carbon-bearing alloys, an η double carbide were distributed as a series of dots outlining primary nickel.

Effect of Composition

Cobalt-10 Aluminum - Figure 7 represents the unmodified structure of the cobalt-10 aluminum eutectic. As etched the brittle cobalt aluminum intermetallic appeared as a dark continuous network around islands of cobalt. Before etching, however, the CoAl appeared pink, which distinguished it from the white cobalt. Although the macrostructure was columnar, the appearance of the cobalt phase was only slightly dendritic. It is likely, nonetheless, that the islands of cobalt that appeared discontinuous in the microsection were, in three dimensions, continuous through a dendrite spine.

Neither 0.1 yttrium nor 0.5 titanium altered the continuous network of the CoAl, but the titanium made the macrostructure equiaxed. An addition of 0.1 boron coarsened the CoAl and made it appear discontinuous. However, it formed a eutectic constituent that solidified on and between the rounded CoAl constituent so that the continuity of a brittle phase was maintained. Primary dendrites of α cobalt became evident after an addition of 0.1 carbon, and a third phase probably a double carbide appeared in the cobalt dendrites as a fine precipitate. The effect of the complex addition of 0.1 each boron, carbon, titanium, and zirconium was similar to that of a 0.1 boron except more third phase was evident.

The microstructure of the 1.0 carbon modified cobalt-10 aluminum alloy in which CoAl was almost entirely replaced by a

double carbide phase Co_3AlC_x (33) is shown in Figure 8. The rounded areas are primary dendrite arms of cobalt. These are surrounded by a somewhat lamellar cobalt-carbide eutectic constituent which has an appearance deceptively similar to portions of the CoAl network eutectic of the unmodified alloy. The dark etching grain boundary phase is CoAl. In the unetched condition the carbide was observed to have a deeper pink hue than the CoAl. After etching the carbide remained pink while the CoAl darkened as it did on etching in the unmodified binary.

The distribution of the carbide was discontinuous. In addition to being present in the eutectic constituent between the dendrite arms, it was also present within the primary cobalt as a particulate precipitate. The particles ranged from rounded to polygonal shapes that were primarily hexagonal idiomorphs. The edges of the hexagons in any one grain tended to be parallel and there was also a suggestion of crystallographic alignment in the arrangement of the particles in the matrix.

Cobalt-42 Chromium - All but one of the cobalt-42 chromium alloys had a network type of structure formed by the δ phase; all were strongly dendritic in α cobalt; all were coarsely columnar; and all were brittle. Figure 9 shows the unmodified structure. Only in the 0.1 boron modification was the δ discontinuous. Nonetheless, a continuum of brittle phase was

maintained by a boron-rich eutectic that formed on and between the δ particles. The overall morphology of the 1.0 carbon modified alloy was similar to the 0.1 boron modifications except the δ was replaced by a fine lamellar constituent.

Cobalt-37 Molybdenum - The cobalt-37 molybdenum eutectics usually had an extremely fine lamellar structure. Figure 10 shows the typical morphology of the eutectic constituent. While a central rib grew parallel to the direction of heat flow, the lamellae in some sections were almost at right angles to this direction. The growth pattern appeared to be strongly influenced by the crystal structure of the Mo_6Co_7. The eutectic grains may be considered as fine dendrites of the molybdenum-rich phase in a cobalt matrix. The relationship of the lamellae to the rib appeared to be identical to that found in coarse primary Mo_6Co_7 "dendrites" in some of the modifications.

Cobalt-45 Tungsten - The macrostructure of the unmodified cobalt-45 tungsten was equiaxed and appeared to be determined by random nucleation of the cobalt-tungsten intermetallic phase W_6Co_7. The structure of the eutectic constituent was in many respects similar to that of cobalt-37 molybdenum. This is not surprising in view of the great similarities of their phase diagrams and constituent phases. W_6Co_7 and Mo_6Co_7 are both rhombohedral-hexagonal and isotypic with W_6Fe_7 (26). These compounds are intermediate phases of variable stoichiometry

of the $D8_5$ structure type and are called μ phases (34).

The unmodified microstructure shown in Figure 11 consisted of plates of primary μ near which primary cobalt was nucleated. Since no crystallographic orientation relationship determinations were made, it is not possible to say whether the primary cobalt merely nucleated on pre-existing heterogeneous nuclei when the regions surrounding the tungsten-rich plates became enriched in cobalt, or whether they nucleated on the W_6Co_7 plates. Every plate of W_6Co_7 was surrounded by a region of primary cobalt. Secondary dendrite arms of cobalt grew from many of the "halos" of cobalt surrounding the W_6Co_7 plates while the remaining volume was filled with a lamellar eutectic constituent. A continuity of the cobalt lamellae of the eutectic with the primary cobalt was evident from a continuity of striations of a widmanstätten precipitate in the cobalt phase that could be seen in heavily etched samples of the cobalt-45 tungsten alloys. This continuity suggests that the eutectic was nucleated by the cobalt phase.

The eutectic was most frequently lamellar, but as can be seen in Figure 11b some W_6Co_7 appeared rod-like. The crystal structure of the W_6Co_7 phase like Mo_6Co_7 exerted a strong influence on the shape of the eutectic. Instead of growing parallel to the direction of heat flow, the lamellae formed a pattern like a feather. A central rib, representing the shaft pointed in the direction of growth. The lamellae, representing

the barbs, made an acute angle with the shaft toward the direction of growth. This pattern was also adopted by some relatively coarse primary dendrites of W_6Co_7 in the cobalt-tungsten system.

The lamellar eutectic (seen in Figure 11) was present in all the alloys except the 1.0 titanium modification and the 0.1, 0.5 and 1.0 carbon modifications. The addition of 0.1 carbon resulted in many small primary μ phase plates with virtually no eutectic. The addition of 1.0 titanium resulted in a much coarser structure where primary μ adopted the feather pattern of the eutectic constituent but on a grosser scale. Both of these structures in which the eutectic was lacking were equiaxed. When the 0.5 and 1.0 carbon additions were made the Co-μ eutectic was replaced by a Co-η carbide eutectic. In these modifications the primary μ was also replaced by primary η .

The addition of 0.1 boron resulted in many coarse eutectic cells and few primary W_6Co_7 plates, with a boron-rich eutectic joining the μ phase lamellae of the eutectic. Magnesium, calcium, yttrium, titanium and aluminum additions changed the unmodified structure in degree but not in kind. In those instances where the macrostructure was equiaxed the grains appeared to nucleate on the tungsten-rich phase. In columnar structures the α cobalt dendrites appeared to be the first constituent to nucleate.

The structure of the 0.2 carbon modification which is shown in Figure 12 was dominated by primary cobalt dendrites that grew from the surface of the casting to its center. Very little primary W_6Co_7 was present, although one small plate can be seen in Figure 12c which represents a section from a test bar of this modification. In the interdendritic regions were two eutectics. The first one to freeze was typical of the Co-W_6Co_7 feather pattern found in the unmodified eutectic. The other was a Co-η carbide eutectic. Both eutectics can be seen in Figure 12b. The η appeared to have two morphologies: one a fish-bone pattern which was also present in an 0.5 carbon modification and was similar to a constituent identified as η by Rautala and Norton (35); the other was similar to the feather pattern of the W_6Co_7. The fine fish-bone lamellae were observed to grow directly from the coarser relatively straight lamellae that had the same external shape as the W_6Co_7 lamellae. The coarse lamellae of η had speckled surfaces that may have been due to the precipitation of small volumes of cobalt solid solution in lamellae that had solidified as W_6Co_7. The η lamellae appeared to be continuous with the lamellae of W_6Co_7 that had unbroken surfaces except for grain boundaries between the two phases present in a single lamella that were observed after agressive etching. This etching also revealed the widmanstatten pattern in the cobalt matrix referred to earlier. It was probably the result of the precipitation of Co_3W (36) and was particularly evident in slowly

cooled castings.

Nickel-37 Tantalum - The unmodified nickel-37 tantalum eutectic (Figure 13) was characterized by large thin plate-like dendrites of primary $TaNi_3$. They were evident as needles, some over 1/2 inch long, extending across the polished sections. That they were in fact plates was evident from an examination of the self decanted surfaces found in shrink holes. Free standing $TaNi_3$ plates that looked like two-dimensional dendrites had substantial central ribs but tapered to feather edges. Their growth appeared to be completely random, independent of the growth of the nickel matrix and of each other. Even at grain boundaries in the matrix there was little that could be considered as a eutectic structure. Only when carbon or boron additions were made, did the nickel-37 tantalum alloys contain a significant eutectic constituent. Carbon resulted in small amounts of a script-like eutectic constituent and boron formed a fine lamellar eutectic on the $TaNi_3$ plates. None of the other additions had a significant effect either on the primary $TaNi_3$ plates nor formed a eutectic constituent.

The addition of 0.1 percent carbon had little effect on the overall structure. It did, however, introduce a new phase presumably the hexagonal tantalum carbide Ta_2C. Kuo has stated that tantalum does not form a double carbide with nickel, although it does form triple carbides (37). Small hexagonal idiomorphs of the new phase were almost randomly dispersed in

both phases, being only slightly smaller and less concentrated in the plates of primary $TaNi_3$ than in the nickel matrix. From this, one would conclude that the carbide nucleated neither primary nickel nor $TaNi_3$, and was present as a proeutectic solid before either of the other phases started to solidify.

The addition of one percent carbon altered the structure drastically by completely eliminating the plate-like phase. The modified structure is shown in Figure 14. The plates of $TaNi_3$ plates were replaced by compact idiomorphs of Ta_2C.

The randomly dispersed carbides occurred as polyhedral idiomorphs. The presence of relatively large carbide particles even at the chill-metal interface (Figure 14a) indicated that some of the carbide was proeutectic. However, particularly in the slowly cooled portion of the melt (Figure 14c), there was evidence of a script-like carbide eutectic constituent. The eutectic adopted a rosette-like pattern (later to be discussed under nickel-tungsten) wherein a primary carbide particle at the center was surrounded by the nickel-rich matrix phase which in turn was surrounded by the script-like eutectic.

Nickel-45 Tungsten - Nickel and tungsten solid solutions form a eutectic at 45 weight percent tungsten. Its structure is shown in Figure 15. At equilibrium the tungsten-rich phase accounts for about 5 percent of the volume. The unmodified

eutectic structure was largely columnar in the 3/4 inch diameter casting. Primary nickel dendrites extended from the surface almost to the center of the 3/4 inch diameter casting. Around the nickel dendrites was a generally rod-like eutectic which had a limited amount of plate-like tungsten constituent. Where the tungsten rods were parallel to the nickel dendrite arms and both were at right angles to the plane of polish, the nickel matrix of the eutectic was often continuous with the nickel of the primary dendrites, indicating that primary nickel nucleated the eutectic.

As close as 1/8 inch to the surface of the 3/4 inch diameter casting, but predominantly at the 1/4 inch mark were primary tungsten dendrites. These dendrites were rudimentary in that they were limited to simple shapes such as polygons, trefoils, small crosses or cloverleafs. They formed the centers of relatively equiaxed eutectic grains or cells. Usually the central tungsten dendrite was completely separated from the eutectic surrounding it by a region of primary nickel. However, some of the tungsten dendrites had rods or lamellae growing directly from them, as can be seen in Figure 15b. Sometimes, the eutectic tungsten was unmistakeably lined up with the axes of a tungsten dendrite in the center of a rosette. At the center of the 3/4 inch diameter casting in the primary nickel dendrites was a pearlite-like constituent. A grain boundary between the nickel matrix of the "pearlite"

and the primary nickel dendrite in which it formed indicated that it was a cellular precipitate (38) (39). It was not determined whether the precipitating phase was tungsten or WNi_4 which is the phase in equilibrium with nickel solid solution below about 1780°F.

The formation of primary tungsten dendrites was suppressed by the following additions: 0.1 magnesium, 0.1 yttrium, 0.1 lanthanum, 0.1 cerium, 0.1 boron and 0.1 aluminum. The addition of 0.1 titanium or 0.1 zirconium increased the number of primary tungsten dendrites. The nickel-tungsten eutectic was partially replaced by a nickel-carbide eutectic when 0.1 carbon was added. No tungsten phase was evident after an addition of 1.0 carbon.

The boron modified microstructure (Figure 16) was different from the unmodified structure in several respects. Virtually no primary tungsten "dendrites" were present. The macrostructure was more columnar and the primary nickel dendrites were much finer and more uniform than in the unmodified castings. The tungsten eutectic constituent, however, was coarser and more rounded and was arrayed in a more curved, less geometric, fashion than was true for the unmodified eutectic.

As discussed previously the tendency to agglomerate the subordinate (non-matrix) phase was a characteristic of boron in all the systems to which it was added. Small amounts of a dark etching, fine lamellar second eutectic which occurred on

the surface of some of the tungsten particles were presumed to be a boron-rich eutectic.

A further difference between the boron modified and the unmodified structures was a precipitate in primary nickel dendrites, which appeared to be variant of the typical cellular precipitate observed near the center of the 3/4 inch diameter unmodified nickel-tungsten casting. In the boron modified alloy, the precipitate, presumed to be tungsten, was distributed throughout the castings, and was not contained in a clearly defined recrystallized cell. Nonetheless, evidence of recrystallization was detected in the regions of the precipitate when oblique illumination was used.

The structure of the nickel-45 tungsten plus 1.0 titanium alloy shown in Figure 17 was made up of globular particles of tungsten in a matrix of nickel solid solution. The globules of tungsten appeared to be of two types: (1) rudimentary primary tungsten dendrites and (2) a globular eutectic constituent. The globular eutectic constituent could be distinguished from the primary tungsten particles by its somewhat elongated shape and its location at grain boundaries or the heavily cored dendrite cell boundaries. The formation of the rod-like eutectic was entirely suppressed.

The microstructure of nickel-45 tungsten eutectic modified by the complex addition of 0.1 each (boron, carbon, titanium, and zirconium) is shown in Figure 18. The tungsten primary dendrites were completely lacking in this modification just as

they were in the 0.1 boron modification. At a magnification of X100 the microstructure appeared very similar to that of the 0.1 boron modification. At higher magnification, however it was seen that the gross pattern of a tungsten-rich constituent around primary nickel dendrites was formed by a different phase. The rounded script-like tungsten eutectic had been replaced by a discontinuous angular, massive carbide and a fish-bone eutectic, both believed to be the η carbide (40). However, a few small eutectic cells of the script-like tungsten constituent were found concentrated at the surface and center of the 3/4 inch diameter cylindrical casting.

Although one might expect a grain refining effect from carbides and borides of the Group IV elements, titanium and zirconium (27) (28) no such effect was noted. The grains of the casting with the complex addition were relatively coarse and columnar. An examination of the slowly cooled portion of the melt revealed the presence of both forms of the cellular precipitate found in the 0.1 boron modification. However, somewhat less of this constituent was present than in the 0.1 boron modification.

Choice of Compositions to be Tested

Microstructure was used as the basis for selecting the compositions for which mechanical properties would be obtained from the sixty-four exploratory types. The chief criterion

was that the matrix phase appeared to be continuous. Further, the shape of the subordinate phase should not be plate-like. Although rod-like morphologies were tested, the preferred eutectic constituent shape was an equiaxed one. Microstructures with angular to sub-angular constituents were tested providing the shapes were relatively small and equiaxed. The ideal of an extremely fine equiaxed dispersion was not achieved in a cast structure except in a small layer near the chill mold surface, and this layer could not be tested.

Additional criteria used in the evaluation of some of the nickel-tungsten eutectics were the absence of the primary tungsten constituent and a finer constituent size in the eutectic tungsten phase. Finally the distribution of the matrix was considered. Since in many of the structures the matrix was present in a columnar dendritic structure, those structures were sought in which there were no long paths through the matrix uninterrupted by a dispersed phase.

MECHANICAL PROPERTIES

Of the sixty-four exploratory melts made, nine had microstructures which showed promise of improved strength or ductility. These were cobalt-10 aluminum plus 1.0 carbon, cobalt-45 tungsten plus 0.2 carbon, nickel-37 tantalum plus 1.0 carbon and nickel-45 tungsten plus the following additions: 0.1 boron, 1.0 titanium, 0.1 each (boron, carbon, titanium and

zirconium), 0.1 yttrium and 0.1 lanthanum. Melts of these compositions were cast into test bars and were tested in tension at room temperature and stress rupture tested at 1800°F. The results from the first six compositions listed above are summarized in Figures 20 through 25. These figures each show the microstructure at a magnification of X100 (reduced approximately 25% in printing) of an unmodified alloy and of a modified alloy of the same base. They also show 1800°F stress rupture curves and give the results of room temperature tensile tests.

The superior properties of the cobalt-10 aluminum plus 1.0 carbon modification are shown in Figure 20. At 1800°F and 5000 psi the modified alloy had a life of 168 hours compared to 7.3 hours for the unmodified. At 1800°F and 15,000 psi, a specimen with a 0.1 hour life had over 80 percent elongation. On the basis of hardness, R_C 32.5 unmodified and R_C 23.0 modified, one would expect better tensile strength for the unmodified alloy. However, because of low ductility (less than 1.0 percent elongation) the true ultimate strength of the unmodified alloy was not reached. As a result the more ductile (3.5 percent elongation) modified specimens reached a higher ultimate tensile strength, 100,400 psi compared to 77,000 psi for the unmodified alloy. The tensile fracture of the unmodified showed cleavage facets while the carbon modified alloy had a fibrous dendritic fracture.

The improved properties resulting from the 0.2 carbon modification of the eutectic cobalt-45 tungsten are shown in Figure 21. The ultimate tensile strength was 102,200 psi and the elongation was less than one percent. The average stress rupture life was only 5.4 hours and the average elongation was 26 percent at 15,000 psi and 1800°F. After the addition of 0.2 carbon the stress rupture properties at 1800°F were considerably improved; the average life at 15,000 psi was 38 hours and the elongation was 10.5 percent. Although room temperature tensile strength was increased to 125,000 psi the elongations remained low, less than one percent. The hardness of the modified and unmodified alloys were virtually the same R_c 49.5 and 49.0 respectively.

Figure 22 shows that the 1.0 carbon modified nickel-37 tantalum alloy was slightly better than the unmodified alloy in tensile strength (86,200 psi compared to 74,500 psi) and had an appreciably better life (74 hours compared to 15 hours) at 5000 psi and 1800°F. Its tensile ductility was much improved, 7.5 percent against less than one percent for the unmodified alloy, which fractured by cleavage of the $TiNi_3$ plates. The same type of brittle fracture also occurred in the stress rupture specimens as well. The hardness of the unmodified alloy was R_c 25 while that of the modified alloy was only R_c 14.5

The addition of 0.1 boron improved both the 1800°F stress

rupture properties and the room temperature tensile properties of the nickel-45 tungsten eutectic which are shown in Figure 23. In the unmodified condition the average stress rupture life was approximately 30 hours at 15,000 psi and 1800°F. The ultimate tensile strength was 155,000 psi, but the elongation was less than one percent. The addition of 0.1 boron resulted in a modest increase in stress rupture life at 1800°F. For a stress of 15,000 psi the life was almost double that of the unmodified alloy. The average tensile strength and elongation were increased to 187,500 psi and 4.2 percent respectively. The hardnesses were almost the same, R_c 43 for the unmodified alloy and R_c 44 for the modified.

The best stress rupture properties of any of the alloys tested were exhibited by an alloy of the composition nickel-37 tungsten-.09 boron. This alloy had a life of almost 350 hours at 1800°F and 15,000 psi. This confirms to some extent the contention of Grigorovich (25) that off-eutectic alloys have better high temperature properties than alloys of eutectic composition.

The tensile strength of the nickel-45 tungsten alloy was decreased from 155,000 psi to 121,700 psi by the addition of 1.0 percent titanium but the elongation was increased from less than one percent to five percent. These results are summarized in Figure 24. The 1800°F stress rupture curves of the unmodified and modified nickel-45 tungsten alloys crossed at approximately

20,000 psi and 17.5 hours. At low stresses the modified alloy had a better stress rupture life than the unmodified alloy. For example, at 1800°F and 15,000 psi its average life was 101 hours compared to 30 hours for the unmodified alloy.

The complex addition of 0.1 percent each of boron, carbon, titanium and zirconium increased stress rupture life at 1800°F and improved room temperature tensile ductility, but lowered tensile strength slightly. These results are presented in Figure 25. At a stress of 15,000 psi and a temperature of 1800°F the life was 76 hours compared to 30 hours for the unmodified alloy. The modified tensile strength was 147,500 psi compared to 155,000 psi for the unmodified alloy while the ductility was increased from less than 1 percent to 2.2 percent. The hardness of R_c 41 was nearly the same as the R_c 43 of the unmodified alloy.

MECHANISMS OF MODIFICATION AND EXPLANATION OF STRUCTURAL CHANGES AND PROPERTIES

The mechanism of any solidification process must be considered in terms of nucleation and growth. Modification of a binary eutectic structure can be affected by altering the nucleation or growth characteristics of one or both of the phases. This can sometimes be done without the introduction of a third phase. However, in many of the compositions in this investigation the addition was sufficient to introduce small amounts of a third phase or to replace entirely one of the

phases by another. In this section, mechanisms to account for the structural modifications as well as their effect on properties will be discussed.

Formation of a Third Phase

In five out of the six modifications that exhibited improved properties, a significant amount of a third phase was found. The replacing of the large, brittle plates of $TaNi_3$ by equiaxed idiomorphs of Ta_2C in nickel-37 tantalum and the brittle network of CoAl by a discontinuous double carbide in cobalt-10 aluminum, was accomplished by the addition of 1.0 percent carbon. This resulted in substantial improvements in ductility in both alloys and moderate increases in tensile strength. The improved strengths were probably the direct result of the increased ductility, since hardness measurements of both alloys indicated that the unmodified alloys should be the stronger. The unmodified alloys were probably so brittle that their full tensile strength potential could not be achieved.

An additional but probably minor contribution to their strength came from carbides dispersed in the solid solution matrix of each of these alloys. Although present as a eutectic constituent in cobalt-45 tungsten and nickel-45 tungsten to which small additions of carbon were made, M_6C carbide particles were relatively well dispersed where they could also contribute to the general strength of the alloys. The single additions of boron as well as carbon resulted in the formation of grain

boundary strengthening constituents that resulted in improved stress-rupture properties.

The combined addition of boron, carbon, titanium and zirconium formed massive η carbides that were too coarse and too angular to provide the combination of room temperature strength and ductility found with the 0.1 boron addition. However, their presence at the grain boundaries contributed to this alloy's greater stress rupture life.

Control of Nucleation

Boron and titanium exerted opposite effects on the formation of nuclei of the primary tungsten phase in the nickel-45 tungsten alloys. Increasing additions of titanium increased the number of rudimentary primary tungsten dendrites found, as shown in Figure 30. The particulate eutectic constituent which was also found will be discussed under "growth". The number of particles competing for the available tungsten favored a smaller, less developed primary tungsten constituent. In contrast, boron almost entirely suppressed the formation of primary tungsten dendrites that was observed in the unmodified nickel-45 tungsten; as a consequence, more tungsten was available to form a eutectic constituent.

The structures resulting from these two additions were similar, although achieved by different means. The tungsten occurred as rounded or globular particles in a nickel solid solution matrix and resulted in substantial improvement in

ductility over the rod-like tungsten phase in the unmodified alloy. Both alloys formed precipitates which resulted in improved high-temperature strength. In the boron modification, a cellular precipitate occurred shortly after solidification and was available to increase room temperature tensile strength as well as stress rupture life. In the titanium modification, a general precipitate occurred during testing at 1800°F and increased stress rupture life at low stresses. A general precipitate that may have contributed to its stress rupture life was also observed in the matrix of the cobalt-45 tungsten 0.2 carbon modification, after testing, in greater amounts than observed in the unmodified alloy.

Control of Growth

Growth of a eutectic can be controlled directly by the growth restricting effect of a modifying element concentrated at the solid-liquid interface of a growing phase. Growth can be indirectly controlled by changes in surface energy that determine the shape of the interface or by selective constitutional supercooling that permits one phase to grow at the expense of another.

The structure of the cobalt-45 tungsten plus 0.2 carbon alloy is believed to be the direct result of carbon concentrations at the interface restricting the growth of W_6Co_7 by interferring with the transport of cobalt and tungsten atoms across the solid-liquid interface. As a result, the melt under-

cooled sufficiently for primary cobalt to be nucleated at the surface of the casting before significant growth of the intermetallic phase had occurred. Since most of the W_6Co_7 formed after the growth of primary dendrites of cobalt, it was present as a dispersed eutectic constituent rather than the large, primary plates found in the unmodified alloy. Although the tensile strength was increased, the increased ductility anticipated from the elimination of the large plate-like primary constituent was not realized. The lack of ductility is attributable to an embrittling widmanstätten precipitate (probably Co_3W (36)) in the matrix.

Boron and titanium additions to the nickel-45 tungsten alloy are believed to have produced a globular eutectic constituent by increasing the surface energy. The greater the surface energy of the phase boundary between two constituents of a eutectic, the greater is the tendency for a lamellar eutectic to become globular. Surface energy effects as well as competition for available tungsten may have also contributed to the formation of the rounded, rudimentary primary dendrites found in the nickel-45 tungsten plus 1.0 titanium alloy as compared to the formation of more developed tungsten dendrites in the alloys containing less titanium.

The distribution of coefficients of boron in nickel and tungsten are almost the same, as are the slopes of the liquidus lines of nickel-boron and tungsten-boron phase diagrams (41) (42) so that the conditions for selective constitutional super-

cooling do not exist. On the other hand, titanium does meet the criteria for a solute to cause selective constitutional supercooling in the nickel-45 tungsten eutectic (26). Although general constitutional supercooling would increase the likelihood of nucleating a second phase in advance of a growing dendrite arm, selective constitutional supercooling would be more likely to produce a globular eutectic constituent. Nonetheless, a globular tungsten eutectic constituent was found in the nickel-45 tungsten alloys after the addition of either 0.1 boron or 1.0 titanium. It is believed that its formation was related to a tendency for the rod-like eutectic constituent of the unmodified alloy to thicken on approaching a grain boundary. Increased thickening of rod ends was a characteristic effect of small titanium additions. In some instances, the rods near the grain boundaries appeared to have been pinched off by the nickel matrix and to have become globules; both conditions are typical of what has been observed in other eutectic systems (43) (44).

SUMMARY

The results of stress rupture testing of four different high temperature eutectic compositions has indicated that modification is capable of producing appreciable improvements in these properties. All stress rupture tests were conducted at 1800°F in air. When the cobalt-10 aluminum and nickel-37 tantalum alloys were tested at an initial stress of 5000 psi, additions of one percent carbon resulted in improvements in stress rupture lives of up to 23 times. When the cobalt-45 tungsten and nickel-45 tungsten alloys were tested at an initial stress of 15,000 psi, the additions of small amounts of modifiers such as boron, carbon and titanium increased the stress rupture life a maximum of six times. While the combinations of stress-temperature-rupture life conditions that can be achieved by these modified eutectic alloys are still below the optimum attainable in cast superalloys, the utilization of modification to improve cast eutectic structures and stress rupture properties of cast superalloys appears feasible.

In general the improvement in stress rupture properties obtained with modification was accompanied by improved room temperature ductility. The carbon modification of the cobalt-10 aluminum and nickel-37 tantalum eutectic resulted in appreciable improvement in tensile elongation and also a smaller increase in tensile strength; carbon modification of the cobalt-45 tungsten eutectic did not improve tensile ductility, but increased the

tensile strength. Modification of the nickel-45 tungsten eutectic with small amounts of boron and titanium also improved tensile ductility.

These improvements in mechanical properties were accomplished by altering the shape, distribution and type of phases present in the cast structure. The stress rupture life and tensile strength of the cobalt-10 aluminum, nickel-37 tantalum and nickel-45 tungsten alloys were increased by obtaining a more finely dispersed secondary phase in the primary matrix. In the case of these as well as the cobalt-45 tungsten eutectics, the stress rupture properties were also improved by the formation of borides or carbides at the grain boundaries. The ductility was increased by producing subordinate phases of a more equiaxed structure and a more random dispersion in the matrix.

The mechanisms by which the structures were altered by modification appear to be control of: the phases which solidified, the number of nuclei for these phases and their growth conditions. The substitution of a carbide for a binary intermetallic phase resulted in the modification observed in the cobalt-10 aluminum and the nickel-37 tantalum eutectics. The modification of the cobalt-45 tungsten alloy appeared to be the result of growth restriction of the eutectic phases. The modification of the nickel-45 tungsten eutectic was apparently accomplished by both controlling the presence of nuclei and the conditions of growth.

REFERENCES

1. Plumb, R. C. and Lewis, J. E.: The Modification of Aluminum-Silicon Alloys by Sodium. J. Inst. of Metals, vol. 86, 1957-58, pp. 393-400.

2. Thall, B. M. and Chalmers, B.: Modification in Aluminum-Silicon Alloys. J. Inst. of Metals, vol. 77, 1950, pp. 79-97.

3. Morrogh, H. and Williams, W. J.: Graphite Formation in Cast Irons and in Nickel-Carbon and Cobalt-Carbon Alloys. J. Iron and Steel Inst., vol. 155, 1947, pp. 322-371.

4. Chadwick, G. A.: Eutectic Alloy Solidification. Progress in Materials Science, vol. 12, no. 2, 1963.

5. Tiller, W. A.: The Modification of Eutectic Structures. Acta Met., vol. 5, 1957, pp. 56-58.

6. Gwyer, A. G. C. and Phillips, H. W. L.: The Constitution and Structure of the Commercial Aluminum-Silicon Alloys. J. Inst. of Metals, vol. 36, 1926, pp. 283-324.

7. Guertler, G.: Contribution to the Crystallization of Aluminum-Silicon Alloys. Z. Metallkunde, vol. 44, 1953, pp. 503-509.

8. Kissling, R. J. and Wallace, J. F.: Refinements of Aluminum-Silicon Alloys. Foundry, April, 1963, pp. 74-79.

9. Kim, C. B. and Heine, R. W.: Fundamentals of Modification in the Aluminum-Silicon System. J. Inst. of Metals, vol. 92, 1963-64, pp. 367-376.

10. Schulz, E.: Microscopic Study of Grain Refinement of Silumin. Z. Metallkunde, vol. 39, 1948, pp. 123-128.

11. Davies, V. de L. and West, J. M.: Factors Affecting the Modification of the Aluminum-Silicon Eutectic. J. Inst. of Metals, vol. 92, 1963-64, pp. 175-180.

12. Hardy, H. K.: Joint Discussion on Papers by Thall and Chalmers and Ransley and Neufeld. J. Inst. of Metals, vol. 78, 1950-51, pp. 729-733.

13. Archer, R. S. and Kempf, L. W.: Modification and Properties of Sand Cast Aluminum-Silicon Alloys. Trans. AIME, vol. 73, 1926, pp. 581-627.

14. Guillet, L.: The Aluminum-Silicon Alloys and Their Industrial Use. Revue de Metallurgie, vol. 19, 1922, pp. 303-310.

15. Mondolfo, L. F.: Eutectic Solidification, Discussion. J. Inst. of Metals, vol. 93, 1964-65, pp. 233-34.

16. Mondolfo, L. F.: Joint Discussion on Papers by Thall and Chalmers and Ransley and Neufeld. J. Inst. of Metals, vol. 78, (1950-51) pp. 773-736.

17. Tiller, W. A.: Polyphase Solidification. In: Liquid Metals and Solidification. ASM, Cleveland, Ohio, 1958, pp. 276-318.

18. Chadwick, G. A.: Modification of Lamellar Eutectic Structures. J. Inst. of Metals, vol. 91, 1962-63, pp. 298-303.

19. Reinemann, G. N. and Marsh, L. E.: Mechanical Properties of A356 Aluminum Casting Alloys. Metal Progress, vol. 76, no. 1. July, 1959, pp. 80-86.

20. Dyke, R. H.: Modification of Aluminum-Silicon Alloys. AFS Trans., vol. 59, 1951, pp. 28-34.

21. Mascre, C. and Lefebvre, A.: The Solidification of Aluminum-13% Silicon (Alpax) Alloy. Fonderie, vol. 168, 1959, pp. 484-500.

22. Cremens, W. S.: Use of Submicron Metal and Nonmetal Powders for Dispersion-strengthened Alloys. In: Ultrafine Particles, ed. by W. E. Kuhn, John Wiley and Sons, Inc., New York, 1963, pp. 457-478.

23. Gensamer, M., Pearsall, E. B., Pellini, W. S., and Low, Jr., J. R.: The Tensile Properties of Pearlite, Bainite and Spheroidite. Trans. ASM, vol. 30, 1942, pp. 983-1020.

24. Heine, R. W. and Rosenthal, P. C.: Principles of Metal Casting. McGraw-Hill Book Co., Inc., New York, 1955.

25. Grigorovich, V. K.: Composition Diagrams as a Basis of the Theory of Heat Resistance of Alloys. Russian Met. and Fuel, no. 2, Mar.-Apr., 1962, pp. 53-60.

26. Hansen, M. and Andrenko, K.: Constitution of Binary Alloys. McGraw-Hill Book Co., Inc., New York, 1958.

27. Dennison, J. P. and Tull, E. V.: The Application of Grain Refinement to Cast Copper-Aluminum Alloys Containing the Beta Phase. J. Inst. of Metals, vol. 81, 1952-53, pp. 513-520.

28. Dennison, J. P. and Tull, E. V.: The Refinement of Cast Grain Size in Copper-Aluminum Alloys Containing 7-9% Aluminum. J. Inst. of Metals, vol. 85, 1956-57, pp. 8-10.

29. Freche, J. C. and Waters, W. J.: Exploratory Investigation of Advanced-Temperature Nickel-Base Alloys, NASA memo 4-13-59E, 1959.

30. Davies, V. de L.: Mechanisms of Crystallization in Binary Eutectic Systems. J. Inst. of Metals, vol. 93, 1964-65, pp. 10-14.

31. Alexander, B. H.: Discussion of "The Eutectoid Reaction" by Mehl, R. F. and Dubé, A. In: Phase Transformations in Solids, John Wiley and Sons, Inc., New York, 1951, pp. 582-587.

32. Boyles, Alfred: The Structure of Cast Iron. ASM, Cleveland, 1947.

33. Huetter, L. J., Stadelmaier, H. H. and Fraker, A. C.: Concerning the Ternary System Cobalt-Aluminum-Carbon. Metallwissenschaft und Tech., vol. 14, no. 2, Feb., 1960, pp. 113-115.

34. Nevitt, M. V.: Alloy Chemistry of Transition Elements. In: Electronic Structure and Alloy Chemistry, ed. by P. A. Beck, AIME symposium, Interscience Publishers, New York, 1963, pp. 101-177.

35. Rautala, P. and Norton, J. T.: Tungsten-Cobalt-Carbon System. Trans. AIME, vol. 194, 1956, pp. 1045-1050.

36. Adkins, E. F., Williams, D. N. and Jaffee, R. I.: Development of Wrought Cobalt-Tungsten-Base Alloys. Cobalt, no. 8, Sept., 1960, pp. 16-29.

37. Kuo, K.: The Formation of η Carbides. Acta Met., vol. 1, 1953, pp. 301-304.

38. Geisler, A. H.: Precipitation from Solid Solutions of Metals. In: Phase Transformations in Solids, John Wiley and Sons, Inc., New York, 1951, pp. 387-544.

39. Turnbull, D.: Theory of Cellular Precipitation. Acta Met., vol. 3, Jan., 1955, pp. 55-63.

40. Whitehead, K. and Brownlee, L. D.: Ternary Phase in the System Nickel-Tungsten-Carbon. Planseeber. Pulvermet, vol. 4, 1956, pp. 62-71.

41. Kolomytsev, P. T.: Phase Diagram of the System Nickel-Nickel Subboride. Russian Met. and Fuel, no. 3, 1960, pp. 80-83.

42. Goldschmidt, H. J. et al.: Investigation into the W-rich Regions of the Binary Systems W-C, W-B, and W-Be. ASD TDR-62-25, part II, B. S. A. Research Center, Kitts Green, Birmingham, Great Britain, July 1963.

43. Brady, F. L.: The Structure of Eutectics. J. Inst. of Metals, vol. 28, 1922, pp. 369-419.

44. Scheil, E.: Concerning Eutectic Crystallization. Z. Metallkunde, vol. 45, 1954, pp. 298-309.

TABLES

TABLE I. - SUMMARY OF COMPOSITIONS CAST AND RESULTING MICROSTRUCTURES

Modifying addition, weight percent	Ceramic-cast 3/4 inch diameter cylinder			Distribution of brittle phase at chill-metal interface
	Eutectic morphology	Primary phases present	Macrostructure	
Cobalt-10 aluminum				
Unmodified	Network	None	Columnar	Continuous
0.1 Y		None	Columnar	Continuous
0.1 Ti		None	Equiaxed	Continuous
0.1 B		αCo dendrites	Columnar	Particulate
0.1 C		αCo dendrites		Continuous
1.0 C		αCo dendrites		Continuous
0.1 ea. B,C,Ti,Zr	↓	αCo dendrites	↓	Particulate
Cobalt-42 chromium				
Unmodified	Network	αCo dendrites	Columnar	Continuous
0.5 Ti				Continuous
0.1 B				Particulate
0.1 C				Continuous
1.0 C				Continuous
0.1 TiC				Particulate
0.1 ea. B,C,Ti,Zr	↓	↓	↓	Particulate
Cobalt-37 molybdenum				
Unmodified	Lamellar	None	Columnar	Continuous
1.0 Ti		Mo_6Co_7 + αCo	Equiaxed	Particulate
0.1 Zr			a1/4 Col.	Continuous
0.1 B			Columnar	Particulate
0.1 Al	↓	↓	a1/8 Col.	Continuous
1.0 C	Lam-Rod	η carbide	a1/4 Col.	Continuous
0.1 TiC	Lamellar	3 plates of Mo_6Co_7	Columnar	Continuous

[a]Col. = Columnar.

TABLE I. - Continued. SUMMARY OF COMPOSITIONS CAST

AND RESULTING MICROSTRUCTURES

Modifying addition, weight percent	Ceramic-cast 3/4 inch diameter cylinder			Distribution of brittle phase at chill-metal interface
	Eutectic morphology	Primary phases present	Macrostructure	
Cobalt-45 tungsten				
Unmodified	Lamellar	W_6Co_7 + αCo	Equiaxed	Continuous
0.2 Mg	↓	↓	[a]1/8 Col.	Particulate
0.2 Ca			Equiaxed	Particulate
0.1 Ce			[a]1/4 Col.	Continuous
0.1 Y		W_6Co_7	[a]1/8 Col.	Continuous
0.1 Ti		W_6Co_7	[a]1/4 Col.	Continuous
1.0 Ti	None	W_6Co_7	Equiaxed	Particulate
0.1 Zr	Lamellar	W_6Co_7 + αCo	[a]1/4 Col.	Continuous
0.1 B	Lamellar	W_6Co_7	Columnar	Particulate
0.1 Al	Lam-Rod	W_6Co_7 + αCo	[a]1/4 Col.	Continuous
0.05 C	Lamellar	W_6Co_7	[a]1/4 Col.	Continuous
0.1 C	None	W_6Co_7	Equiaxed	Particulate
0.2 C	Lam-Fishbone	αCo	Columnar	Continuous
0.5 C	Fishbone	η carbide + αCo	Equiaxed	Continuous
1.0 C	Fishbone	η carbide	Equiaxed	Particulate
0.1 TiC	Lamellar	W_6Co_7 + αCo	[a]1/8 Col.	Continuous
Nickel-37 tantalum				
Unmodified	None	$TaNi_3$	Equiaxed	Particulate
0.1 Mg	↓	↓	↓	↓
0.1 Y				
0.1 La				
0.1 Zr				
0.1 B				
0.1 Al				
0.1 C				
1.0 C	Globular	Carbide		
0.1 ea. B,C,Ti,Zr	None	$TaNi_3$		

[a]Col. = Columnar.

TABLE I. - Concluded. SUMMARY OF COMPOSITIONS CAST AND RESULTING MICROSTRUCTURES

Modifying addition, weight percent	Ceramic-cast 3/4 inch diameter cylinder			Distribution of brittle phase at chill-metal interface
	Eutectic morphology	Primary phases present	Macrostructure	
Nickel-45 tungsten				
Unmodified	Rod-like	W, Ni	Columnar	Continuous
0.1 Mg	↓	Ni	Columnar	Particulate
0.1 Y		Ni	[a]1/4 Col.	Particulate
0.1 Ce		W, Ni	[a]1/4 Col.	Continuous
0.1 La		Ni	Columnar	Particulate
0.1 Ti		W, Ni	Equiaxed	Continuous
1.0 Ti	Globular	↓	Equiaxed	Particulate
0.1 Zr	Rod-like		Columnar	↓
0.5 Zr	Rod-Glob.		↓	
0.1 B	Rod-Glob.	Ni		
0.1 Al	Rod-like	Ni		
0.1 C	Rod-like and fishbone	W, Ni		
1.0 C	None	η carbide	Equiaxed	
0.1 ea. B,C,Ti,Zr	Rod-like	Ni	[a]1/4 Col.	
Nickel-16 zirconium				
Unmodified	Rod-like	$ZrNi_4$	Equiaxed	Continuous
0.1 C	Rod-like	$ZrNi_4$, Ni	Equiaxed	Continuous
1.0 C	Rod-like	Carbide, Ni	[a]1/8 Col.	Continuous

[a]Col. = Columnar.

TABLE II. - CHEMICAL ANALYSES

Intended composition	Elements determined										
	Co	Ni	Al	Ta	W	B	C	Zr	La	Ti	Y
	Test bars										
Co-10 Al Unmod.	89.44		10.32					0.18			
Co-10 Al + 1.0 C	88.26		10.64				1.0	0.064			
Co-45 W Unmod.	58.70				41.21			0.04			
Co-45 W + 2.0 C	58.20				41.48		0.18	0.13			
Ni-37 Ta Unmod.		62.20		37.72				0.005			
Ni-37 Ta + 1.0 C		62.90		35.59			0.91	0.55			
Ni-45 W Unmod.		57.57			[a]45.12						
					[a]42.39			0.012			
Ni-45 W + 0.1 B		56.75			43.13	0.08		0.015			
Ni-45 W + 0.1 La		58.04			41.81			0.004	0.019		
Ni-45 W + 1.0 Ti		64.15			[a]34.73			0.08		1.0	
					[a]43.77						
Ni-45 W + 0.1 Y		55.85			43.91			0.10			0.009
Ni-45 W + 0.1 ea. (B,C,Ti,Zr)		59.50			40.07	0.18	0.11	0.017		0.15	
Ni-45 W + 0.1 B[b]		62.85			37.04	0.09		0.010			

[a]From opposite ends of test bar.

[b]Melt 242.

TABLE II. - Concluded. CHEMICAL ANALYSES

Intended composition	Elements determined										
	Co	Ni	Al	Ta	W	B	C	Zr	La	Ti	Y
	Exploratory melts										
Co-45 W Unmod.					41.09			<0.005			
Co-45 W + 0.2 C					44.26			<0.005			
Ni-45 W Unmod.					44.22			<0.005			
Ni-45 W + 0.1 B					45.9	0.05	0.18	<0.005			
Ni-45 W + 1.0 Ti					44.95					0.91	
Ni-45 W + 0.1 ea. (B,C,Ti,Zr)					44.50	0.05	0.18	<0.045		0.11	

TABLE III. - AVERAGE MECHANICAL PROPERTIES

Composition		Ultimate tensile strength, psi	Tensile elongation, percent	Hardness, Rockwell C	Stress-rupture life at 1800° F hr and stress indicated
Base alloy	Additions, weight percent				
Co-10 Al	Unmodified	77.0×10^3	<1	32.5	[a]7.3
Co-10 Al	1.0 C	100.4	3.5	23	[a]168.0
Co-45 W	Unmodified	102.7	<1	49.5	[b]5.8
Co-45 W	0.2 C	125.0	<1	49	[b]38.0
Ni-37 Ta	Unmodified	74.5	<1	25	[a]15.0
Ni-37 Ta	1.0 C	86.2	7.5	14.5	[b]74.0
Ni-45 W	Unmodified	155.0	1	43	[b]30.0
Ni-45 W	0.1 B	187.5	4.2	44	[b]58.0
Ni-45 W	1.0 Ti	121.7	5.0	31	[b]101.0
Ni-45 W	0.1 ea. B,C, Ti,Zr	147.5	2.2	31	[b]76.0

[a] 5,000 psi.

[b] 15,000 psi.

TABLE IV. - RESULTS OF STRESS-RUPTURE TESTS IN AIR AT 1800° F

Specimen number	Base alloy	Modifying addition weight, percent	Initial stress, psi	Time to fracture, hr	Elongation, percent
344-4	Co-10 Al	Unmodified	5,000	7.3	50.0
344-2			7,000	1.65	70.0
344-6			15,000	0.1	80.0
345-3	Co-10 Al	1.0 C	5,000	167.9	10.0
345-6			10,000	5.9	8.5
345-4			15,000	0.8	22.0
327-1	Co-45 W	Unmodified	7,500	33.46	42.5
327-3			7,500	[a]24.0	[a]85.0
327-5			10,000	16.35	52.5
327-2			15,000	5.15	27.5
346-3			7,500	45.65	44.0
346-5			10,000	30.0	37.5
346-1			15,000	5.7	25.0
337-3	Co-45 W	0.2 C	15,000	42.5	12.5
337-5			20,000	14.7	17.5
337-4			30,000	3.3	5.0
347-3			15,000	32.85	12.5
347-2			20,000	12.4	12.5
347-4			30,000	2.95	8.0
362-4	Ni-37 Ta	Unmodified	5,000	15.0	3.5
362-5			7,500	4.3	5.0
362-1			10,000	2.4	4.0
362-3			15,000	0.4	5.0
253-2	Ni-37 Ta	1.0 C	5,000	74.0	32.0
253-1			7,500	6.32	25.0
253-3			10,000	2.7	29.0

[a]Interrupted test.

TABLE IV. - Continued. RESULTS OF STRESS-RUPTURE TESTS IN AIR AT 1800° F

Specimen number	Base alloy	Modifying addition weight, percent	Initial stress, psi	Time to fracture, hr	Elongation, percent
241-1	Ni-45 W	Unmodified	13,000	45.95	4.0
241-3			14,850	25.15	4.0
241-2			15,000	30.15	----
241-5			20,000	21.45	2.5
366-2			13,000	31.65	12.5
366-6			15,000	24.7	10.0
366-5			20,000	14.75	9.0
312-2	Ni-45 W	0.1 B	15,000	44.9	11.0
312-1			20,000	30.27	9.0
312-4			20,000	31.0	----
312-6			30,000	9.2	5.0
339-3			15,000	68.8	11.0
339-4			30,000	21.0	9.0
349-6	Ni-45 W	0.1 C	10,000	24.85	2.0
349-1			15,000	14.6	<1
349-2			20,000	9.1	2.0
385-3			10,000	79.3	9.0
385-2			15,000	29.3	10.0
385-1			15,000	31.77	<1
385-4			20,000	8.1	11.0
311-3	Ni-45 W	0.1 La	15,000	25.05	2.5
311-2			15,000	25.5	4.0
311-5			20,000	11.6	4.0
330-6	Ni-45 W	1.0 Ti	15,000	101.35	----
330-1			20,000	16.2	5.0
330-2			20,000	10.1	7.5
330-3			25,000	1.45	2.5
336-6			15,000	101.1	2.5
336-1			25,000	3.1	2.5

TABLE IV. - Concluded. RESULTS OF STRESS-RUPTURE TESTS IN AIR AT 1800° F

Specimen number	Base alloy	Modifying addition weight, percent	Initial stress, psi	Time to fracture, hr	Elongation, percent
338-6	Ni-45 W	0.1 Y	15,000	59.6	6.0
338-3			20,000	26.6	<1
338-4			25,000	11.45	2.5
363-6			15,000	26.2	11.0
363-5			20,000	17.5	5.0
363-1			25,000	9.25	5.0
357-3	Ni-45 W	0.1 each of Ti, Zr,B,C	15,000	51.95	17.5
357-2			20,000	48.1	14.0
357-1			30,000	7.55	12.5
359-6			15,000	96.1	27.5
359-2			20,000	42.95	14.0
359-5			30,000	12.6	12.5
242-4	Ni-37 W	0.1 B	13,000	638.2	5.0
242-1			15,000	349.5	5.0
242-3			20,000	28.5	1.5

TABLE V. - ROOM TEMPERATURE TENSILE RESULTS

Test bar number	Modifying additions, weight percent	Ultimate tensile strength, psi	0.2 percent yield strength, psi	Elongation, percent	Condition of bar (a)
		Cobalt-10 aluminum			
344-5	Unmodified	77.0×10^3	66	<1	A/C
345-5	1.0 C	100.4	69	3.5	A/C
		Cobalt-45 tungsten			
327-4	Unmodified	97.5	-----	<1	A/C
337-1	0.2 C	125	-----	<1	G
346-4	0.2 C	108	-----	<1	G
		Nickel-37 tantalum			
362-2	Unmodified	74.5	-----	<1	A/C
353-1	1.0 C	86.2	60	7.5	A/C
		Nickel-45 tungsten			
241-6	Unmodified	165	-----	<1	A/C
366-4	Unmodified	145.1	125	1.5	G
312-5	0.1 B	188	-----	5	A/C
339-2	0.1 B	187	132.5	3.5	A/C
349-3	0.1 C	116.5	-----	<1	A/C
385-6	0.1 C	129	124	<1	A/C
311-1	0.1 La	149.5	-----	2	A/C
311-6	0.1 La	166.6	132	4.5	G
330-4	1.0 Ti	118.5	-----	4.5	A/C
336-4	1.0 Ti	125	95	5.5	G
338-5	0.1 Y	139.2	125.8	2	G
363-3	0.1 Y	157.2	118	1.5	G
357-4	0.1 ea.	141.5	116	1.5	G
357-5	B, C,	150	116	3	A/C
359-1	Ti, Zr	145	122.8	2	G

[a]A/C = As cast surface; G = ground surface.

FIGURES

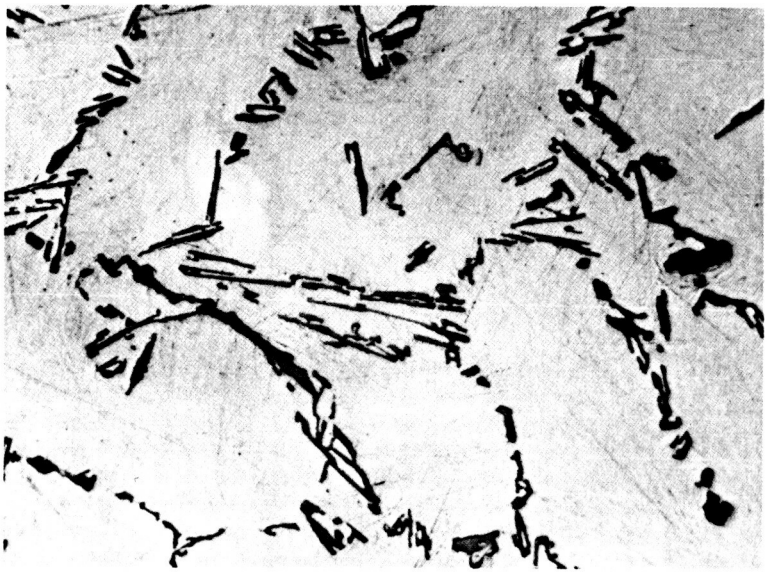

(a) Unmodified.

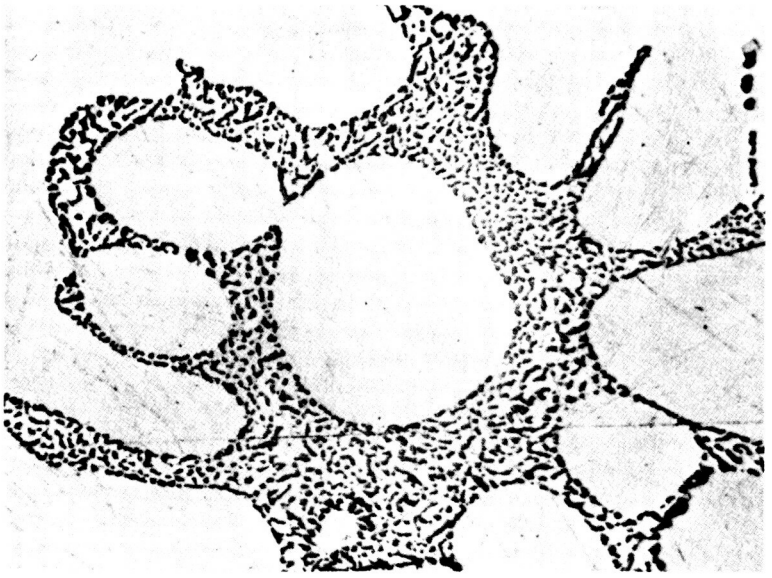

(b) Modified with sodium.

FIG. 1: MICROSTRUCTURE OF ALUMINUM-SILICON EUTECTIC IN A356 ALLOY (A1-7.0 Si-0.3 Mg). 175X. REDUCED APPROXIMATELY 13 PERCENT IN PRINTING.

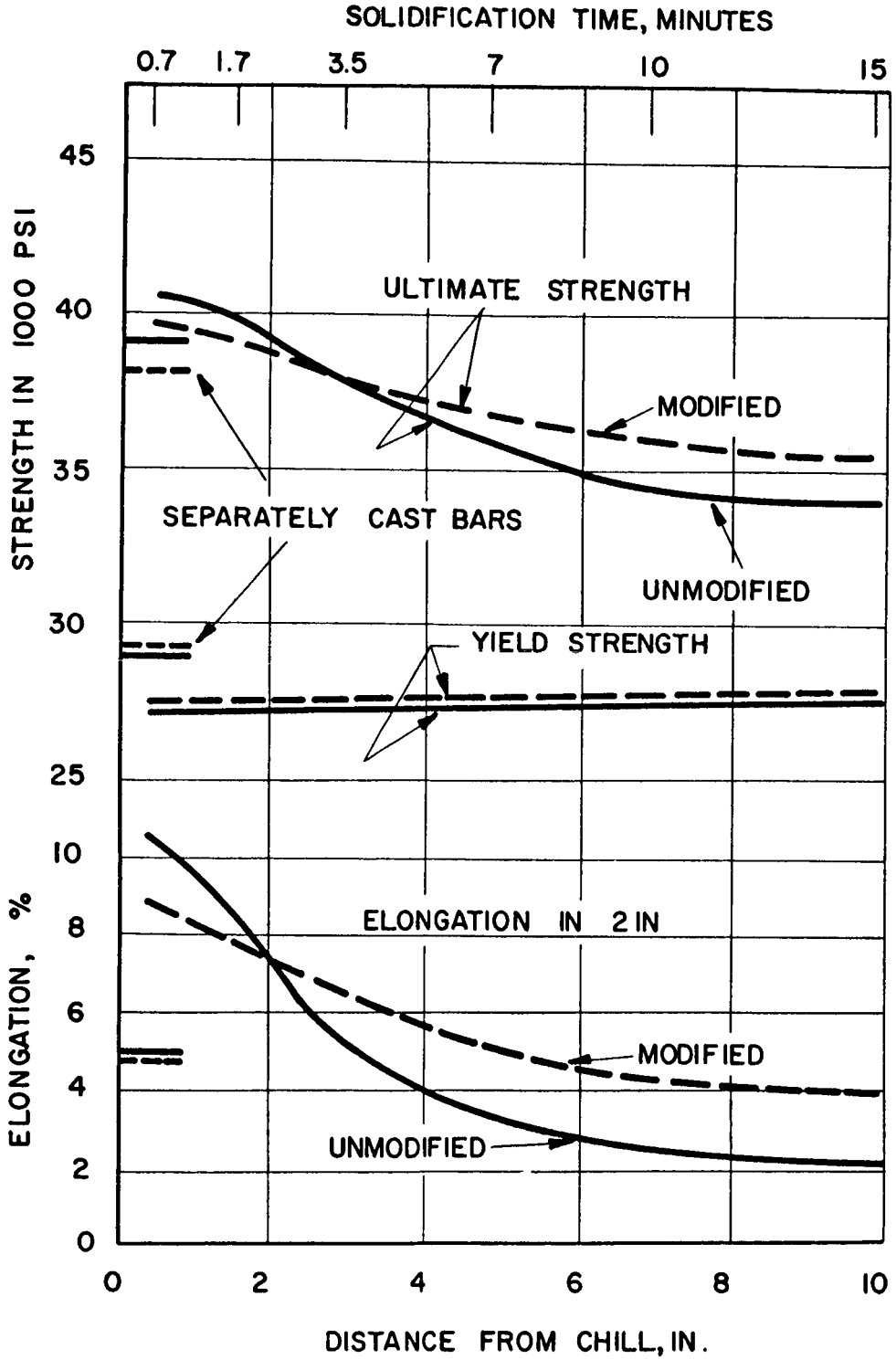

FIG. 2: MECHANICAL PROPERTIES OF A356-T6 (A1-7.0 Si-0.3Mg) BEFORE AND AFTER SODIUM MODIFICATION.

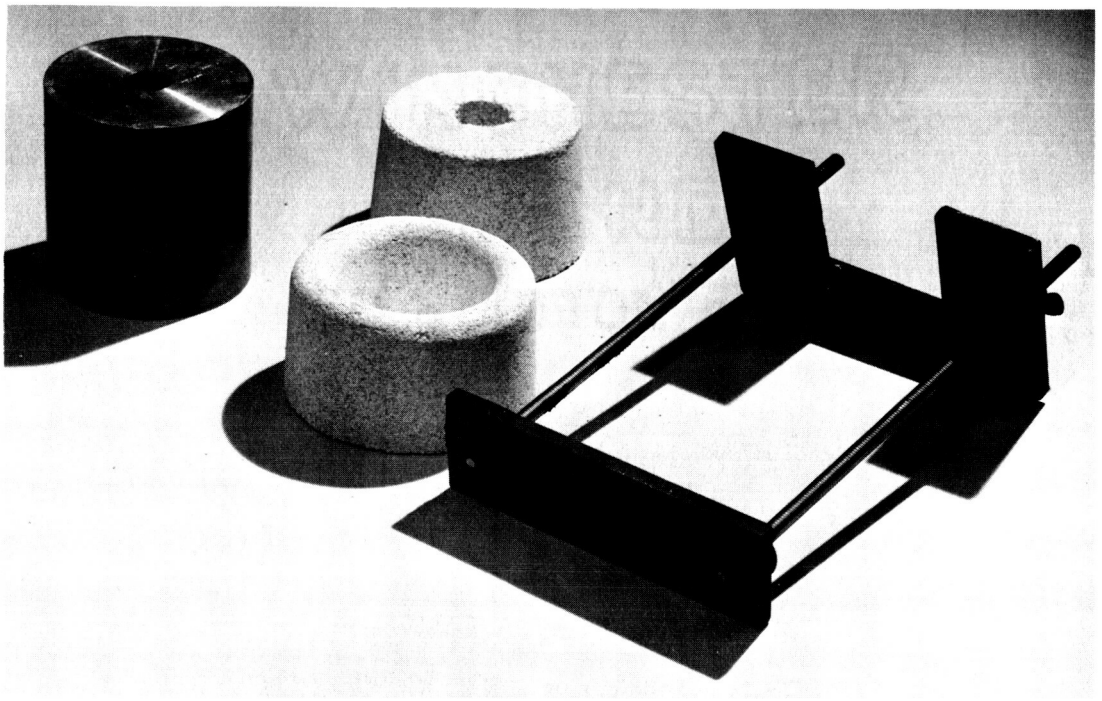

FIG. 3: SECTIONS OF COMPOSITE MOLD, COPPER CHILL MOLD, FUSED SILICA POURING CUP AND MOLD, AND CLAMP.

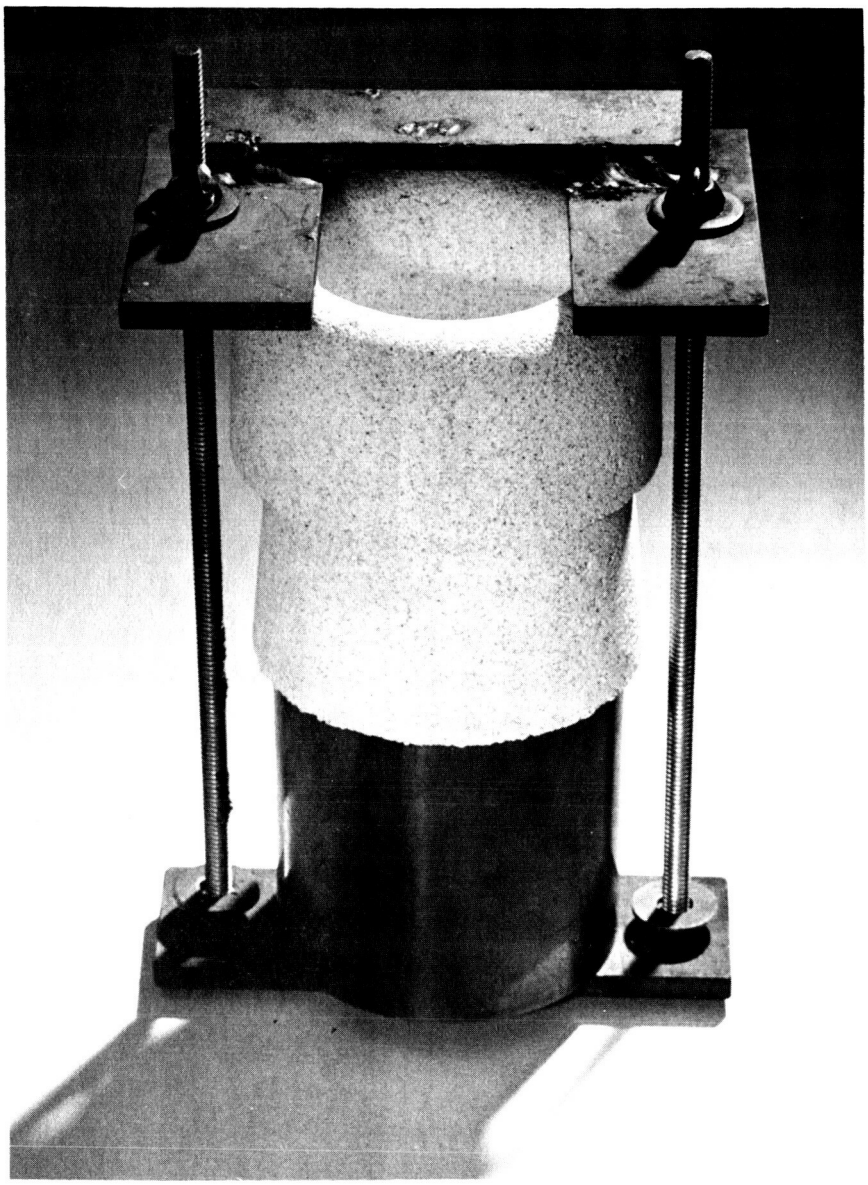

FIG. 4: ASSEMBLED COMPOSITE MOLD SHOWING FUSED SILICA SECTIONS AND COPPER CHILL MOLD.

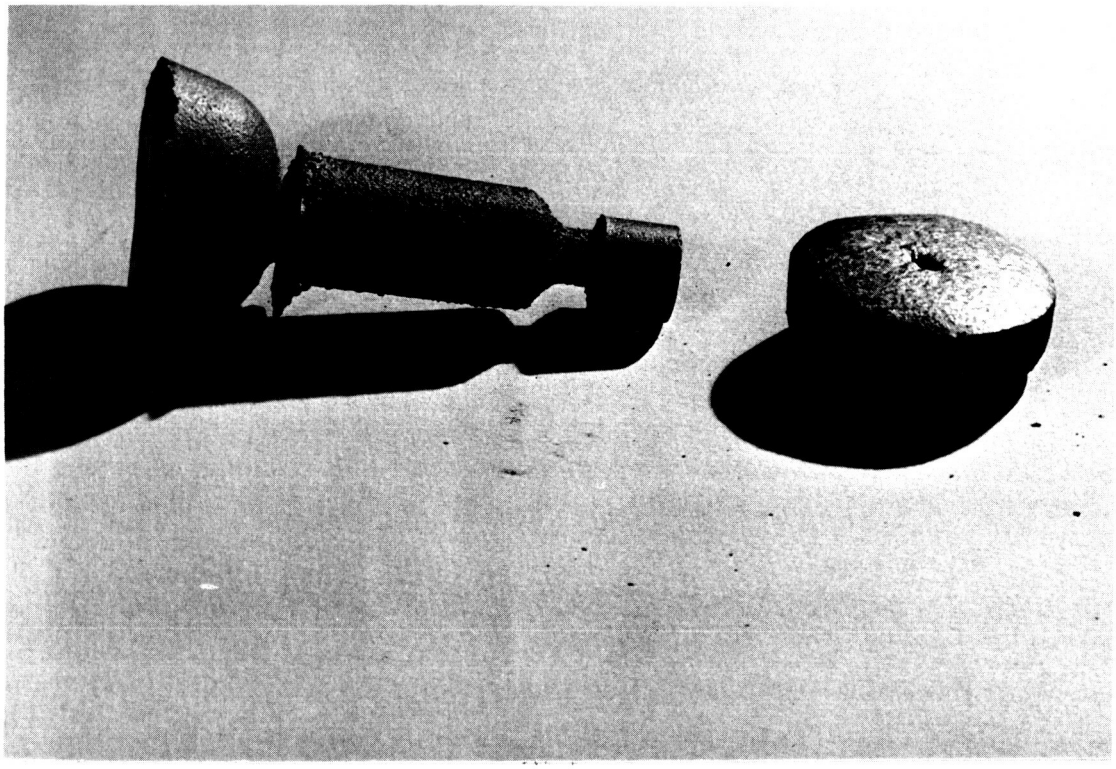

FIG. 5: CASTING FROM COMPOSITE MOLD AND PORTION OF MELT SOLIDIFIED IN CRUCIBLE.

FIG. 6: TEST BAR CASTING AND CERAMIC SHELL MOLD.

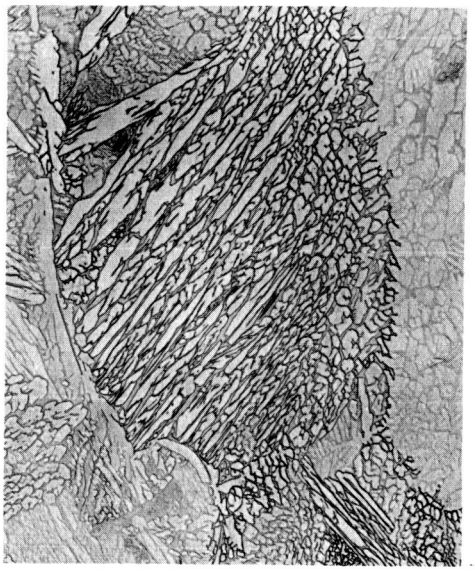

X100

a) Chill Cast

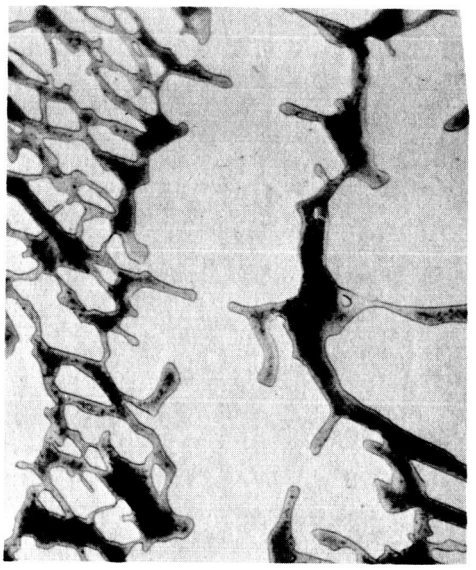

X500

b) Cast in unheated, fused silica mold

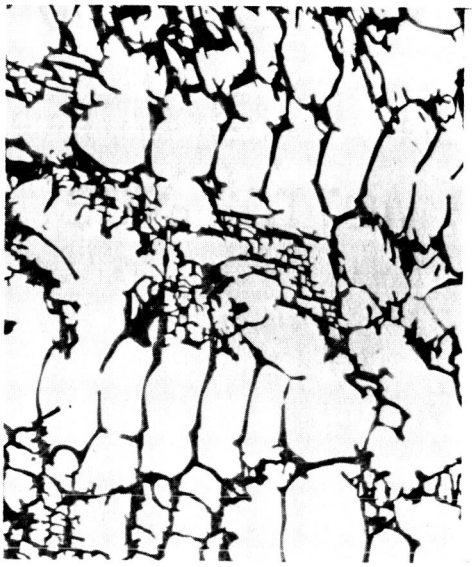

X100

c) Solidified in crucible

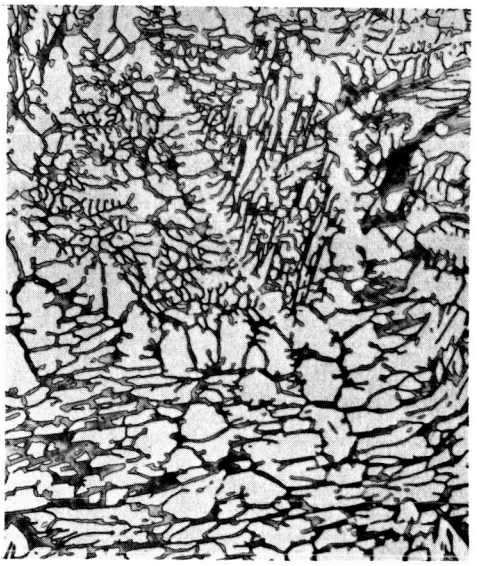

X100

d) Investment cast

Figure 7. Co-10Al unmodified (a,b,c) from same melt cooled at 3 different rates, d) from test bar cast in 1600°F. mold.

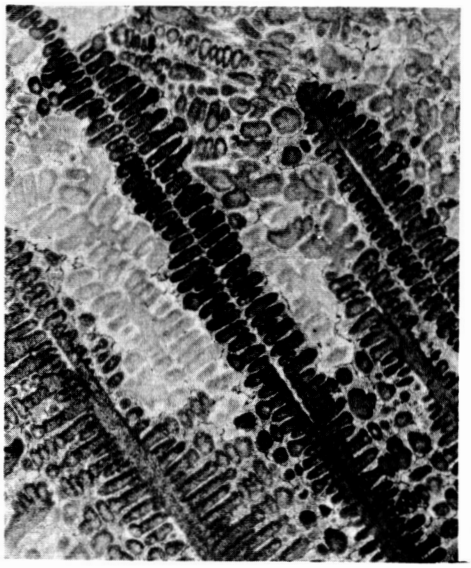

X100

a) Chill Cast

X500

b) Cast in unheated, fused silica mold

X100

c) Solidified in crucible

X100

d) Investment cast

Figure 8. Co-10Al+1.0C (a,b,c) from same melt cooled at 3 different rates, d) from test bar cast in 1600°F. mold.

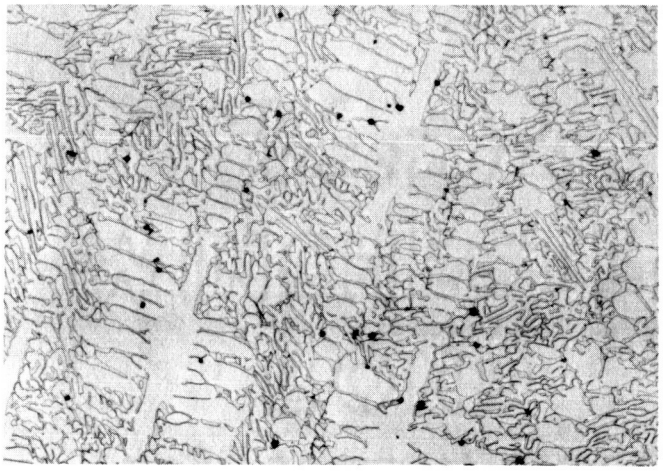

X100

Figure 9. Co-42 Cr, cast in unheated ceramic mold.

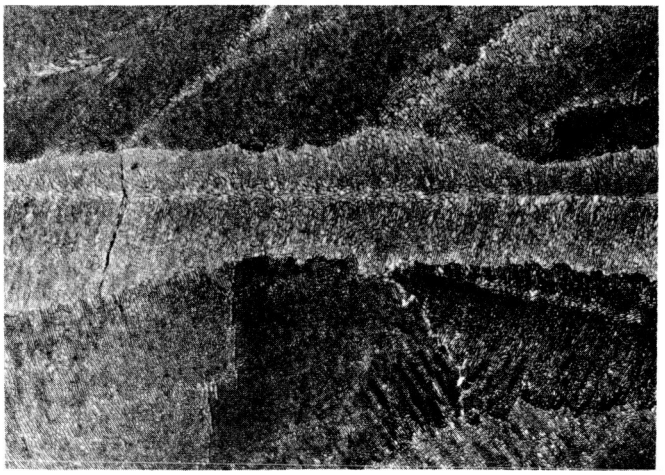

X100

Figure 10. Co-37 Mo, cast in unheated ceramic mold.

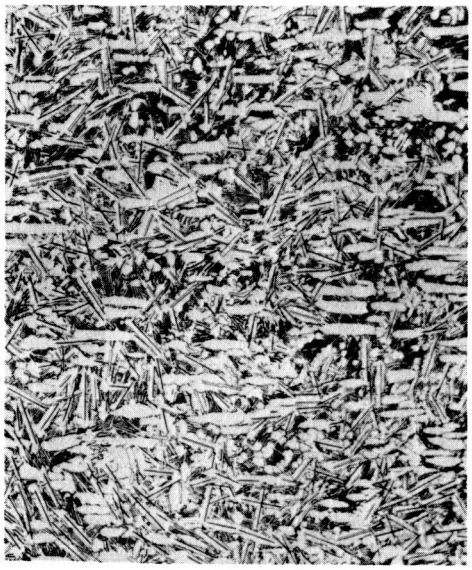

X100

a) Chill Cast

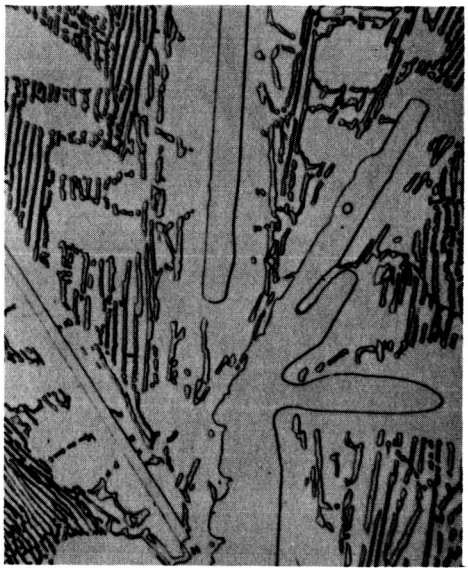

X500

b) Cast in unheated, fused silica mold

X100

c) Solidified in crucible

X100

d) Investment cast

Figure 11. Co-45W unmodified (a,b,c) from same melt cooled at 3 different rates, d) from test bar cast in 1600°F. mold.

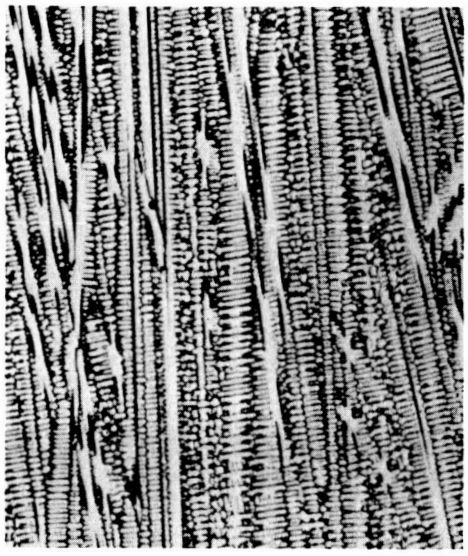

X100

a) Chill Cast

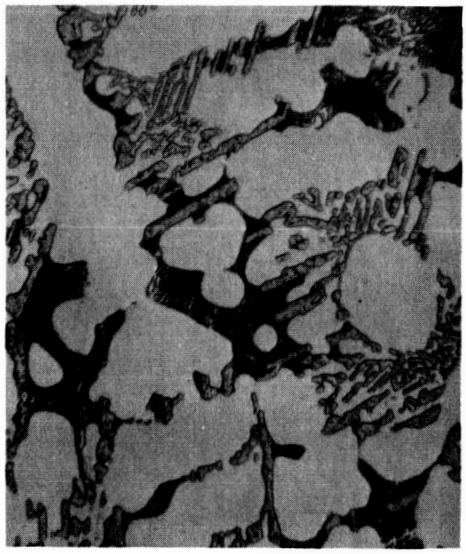

X500

b) Cast in unheated, fused silica mold

X100

c) Solidified in crucible

X100

d) Investment cast

Figure 12. Co-45W+0.2C (a,b,c) from same melt cooled at 3 different rates, d) from test bar cast in 1600°F. mold.

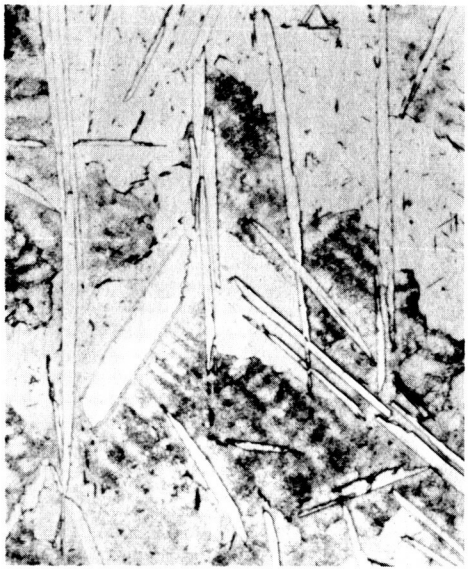

X100

a) Chill Cast

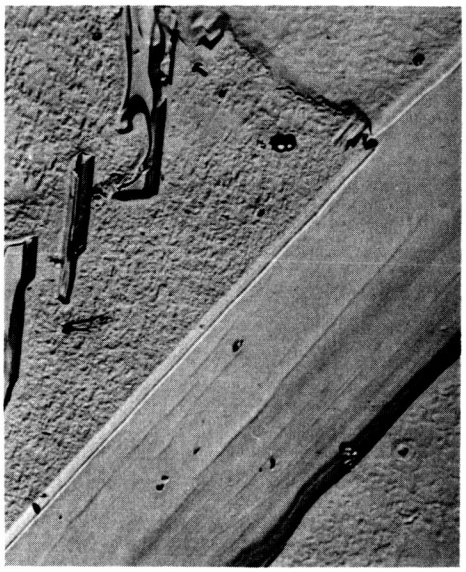

X500

b) Cast in unheated, fused silica mold

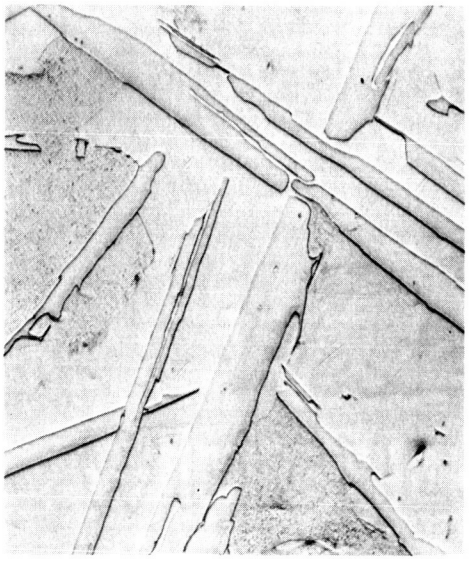

X100

c) Solidified in crucible

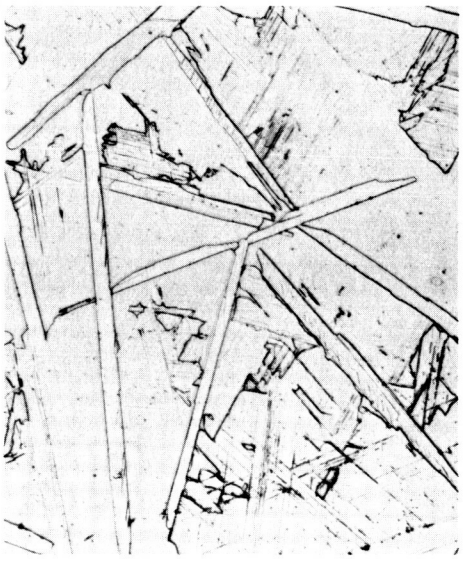

X100

d) Investment cast

Figure 13. Ni-37Ta unmodified (a,b,c) from same melt cooled at 3 different rates, d) from test bar cast in 1600°F. mold.

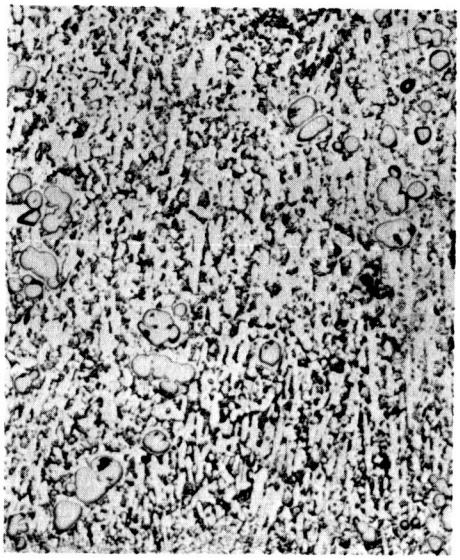

X100

a) Chill Cast

X500

b) Cast in unheated, fused silica mold

X100

c) Solidified in crucible

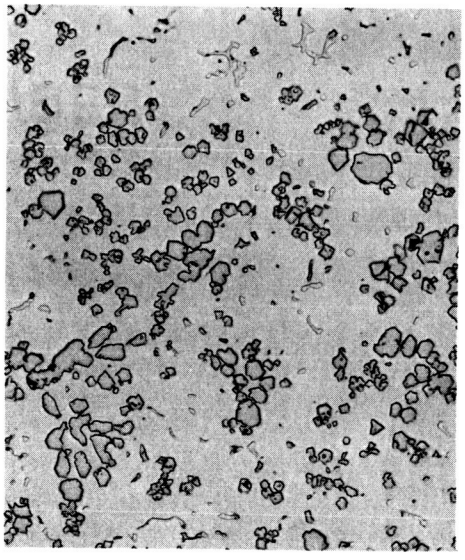

X100

d) Investment cast

Figure 14. Ni-37Ta+1.0c (a,b,c) from same melt cooled at 3 different rates, d) from test bar cast in 1600°F. mold.

X100

a) Chill Cast

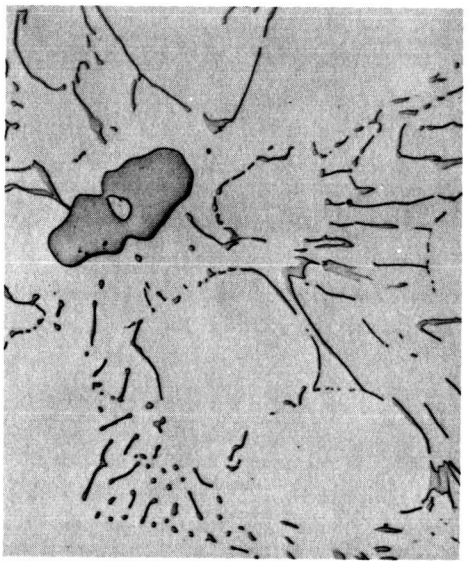

X500

b) Cast in unheated, fused silica mold

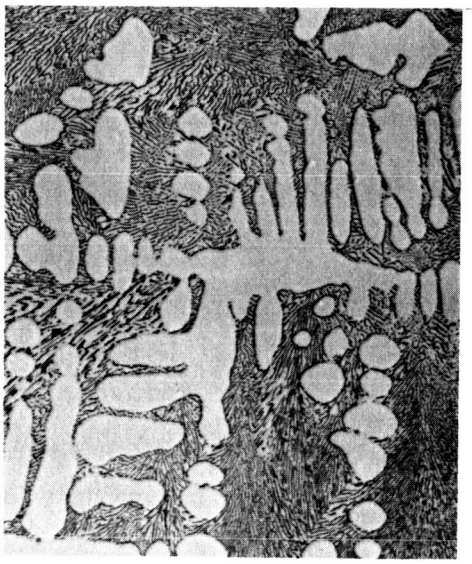

X100

c) Solidified in crucible

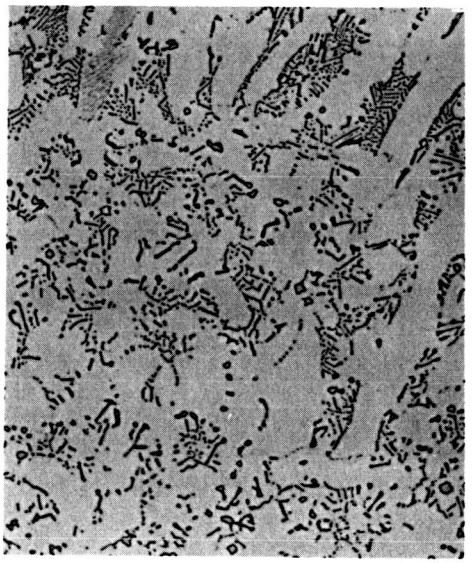

X100

d) Investment cast

Figure 15. Ni-45W unmodified (a,b,c) from same melt cooled at 3 different rates, d) from test bar cast in 1600°F. mold.

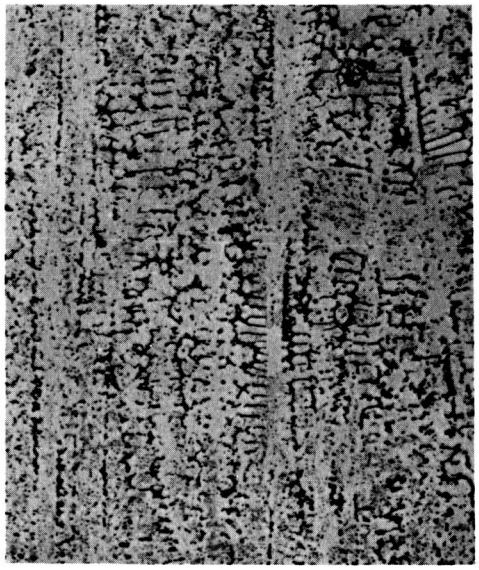

X100

a) Chill Cast

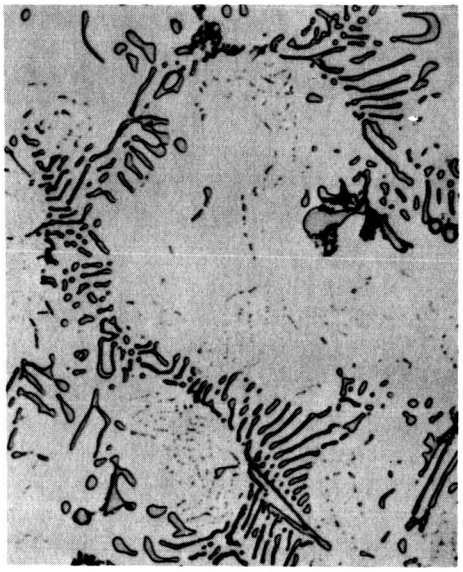

X500

b) Cast in unheated, fused silica mold

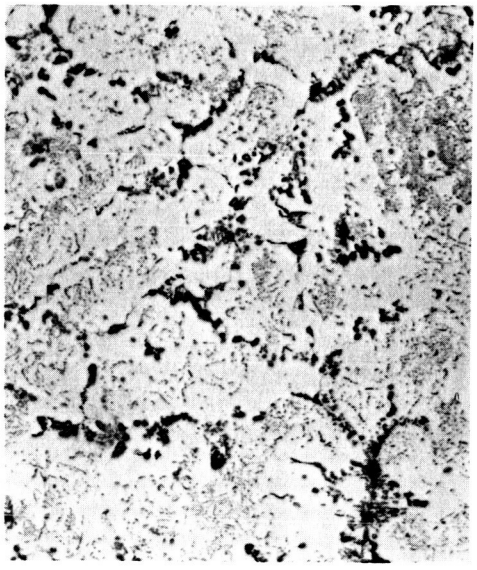

X100

c) Solidified in crucible

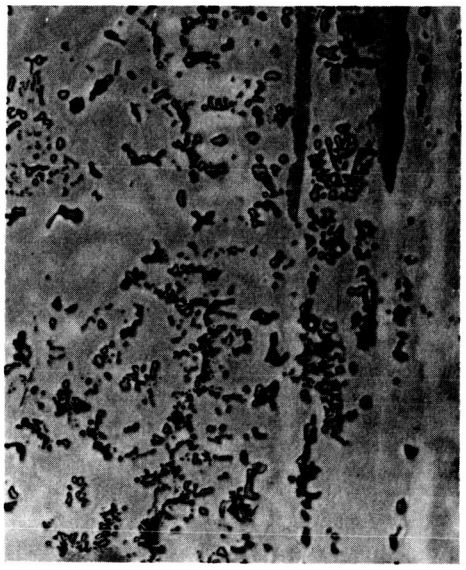

X100

d) Investment cast

Figure 16. Ni-45W+0.1B (a,b,c) from same melt cooled at 3 different rates, d) from test bar cast in 1600°F. mold.

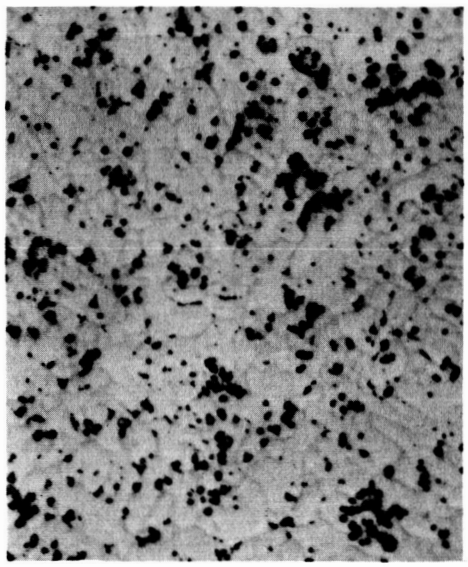

X100

a) Chill Cast

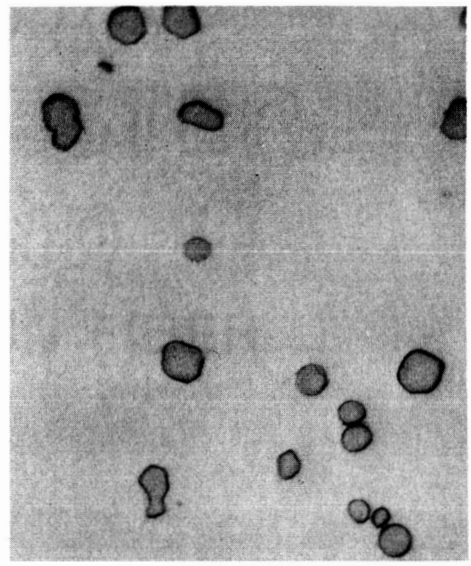

X500

b) Cast in unheated, fused silica mold

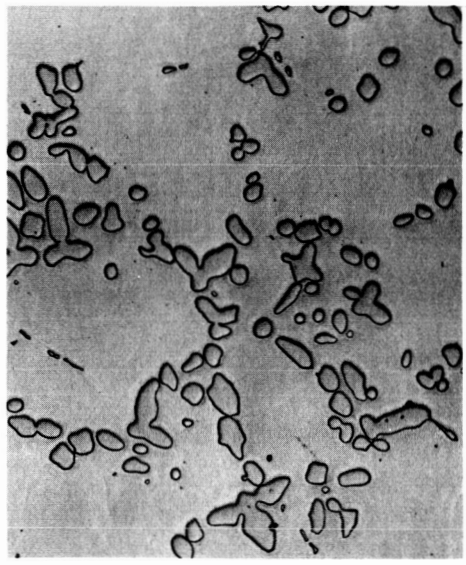

X100

c) Solidified in crucible

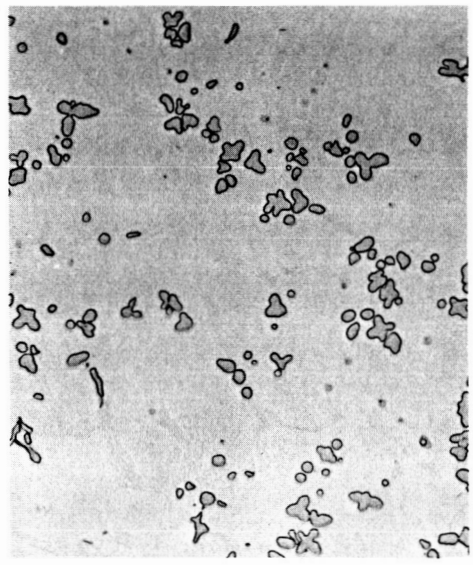

X100

d) Investment cast

Figure 17. Ni-45W+ 1.0Ti (a,b,c) from same melt cooled at 3 different rates, d) from test bar cast in 1600°F. mold.

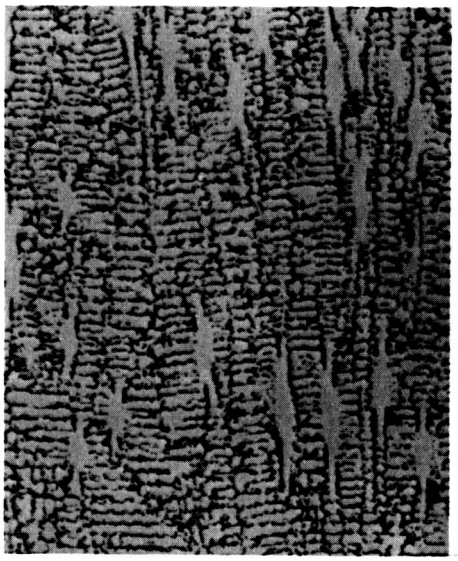

X100

a) Chill Cast

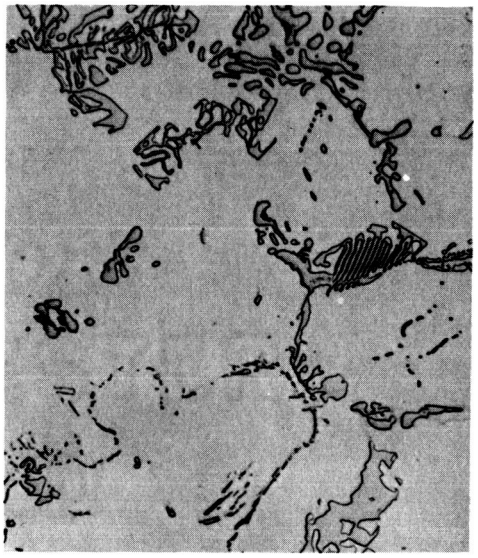

X500

b) Cast in unheated, fused silica mold

X100

c) Solidified in crucible

X100

d) Investment cast

Figure 18. Ni-45W+0.lea.(B,C,Ti,Zr)(a,b,c) from same melt cooled at 3 different rates,d) from test bar cast in 1600°F. mold.

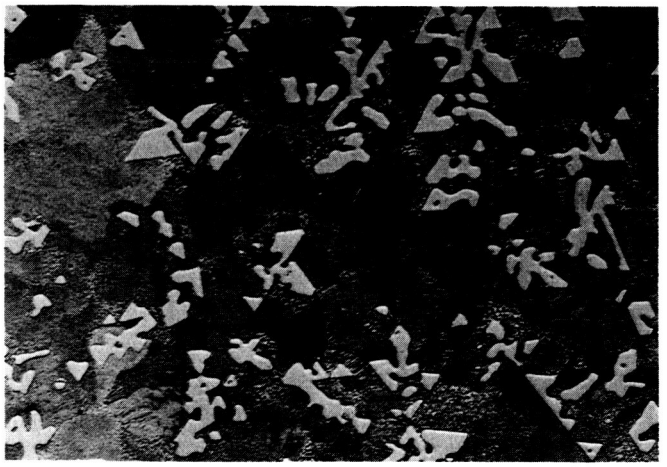

X100

Figure 19, Ni-16 Zr, cast in unheated ceramic mold.

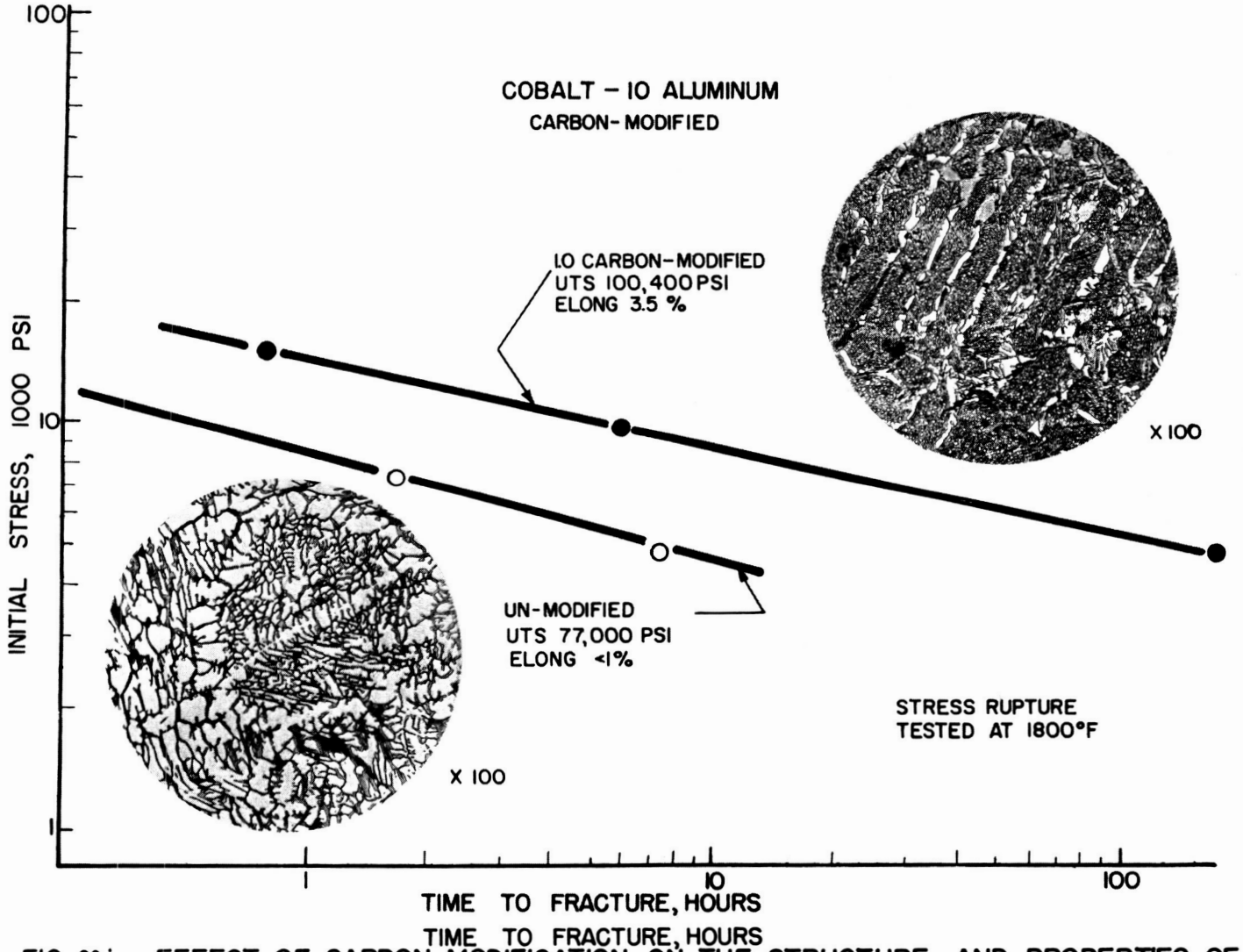

TIME TO FRACTURE, HOURS

FIG. 20: EFFECT OF CARBON-MODIFICATION ON THE STRUCTURE AND PROPERTIES OF THE EUTECTIC ALLOY COBALT-10 ALUMINUM.
REDUCED APPROXIMATELY 27 PERCENT IN PRINTING.

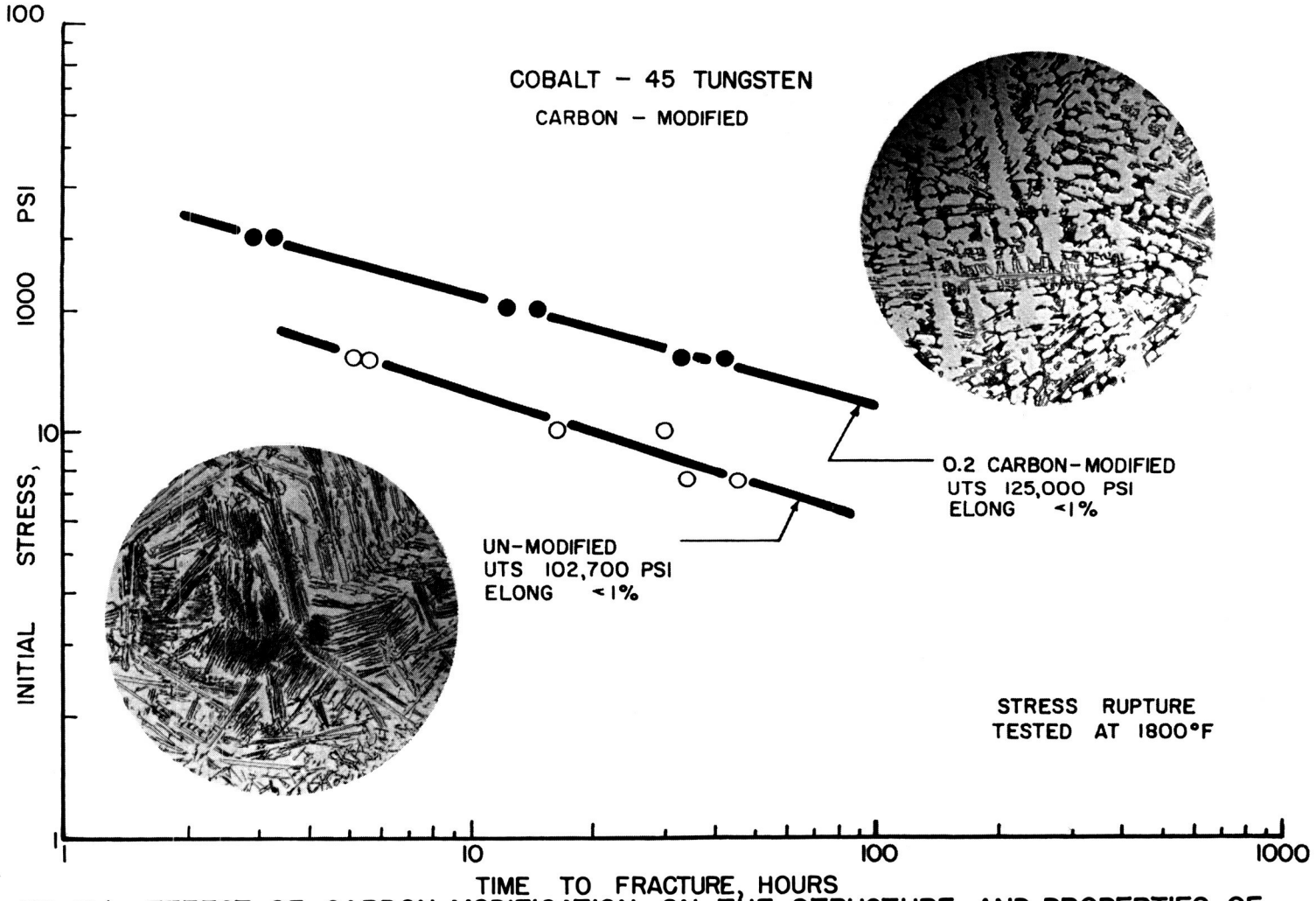

FIG. 21: EFFECT OF CARBON-MODIFICATION ON THE STRUCTURE AND PROPERTIES OF THE EUTECTIC ALLOY COBALT-45 TUNGSTEN.
REDUCED APPROXIMATELY 26 PERCENT IN PRINTING.

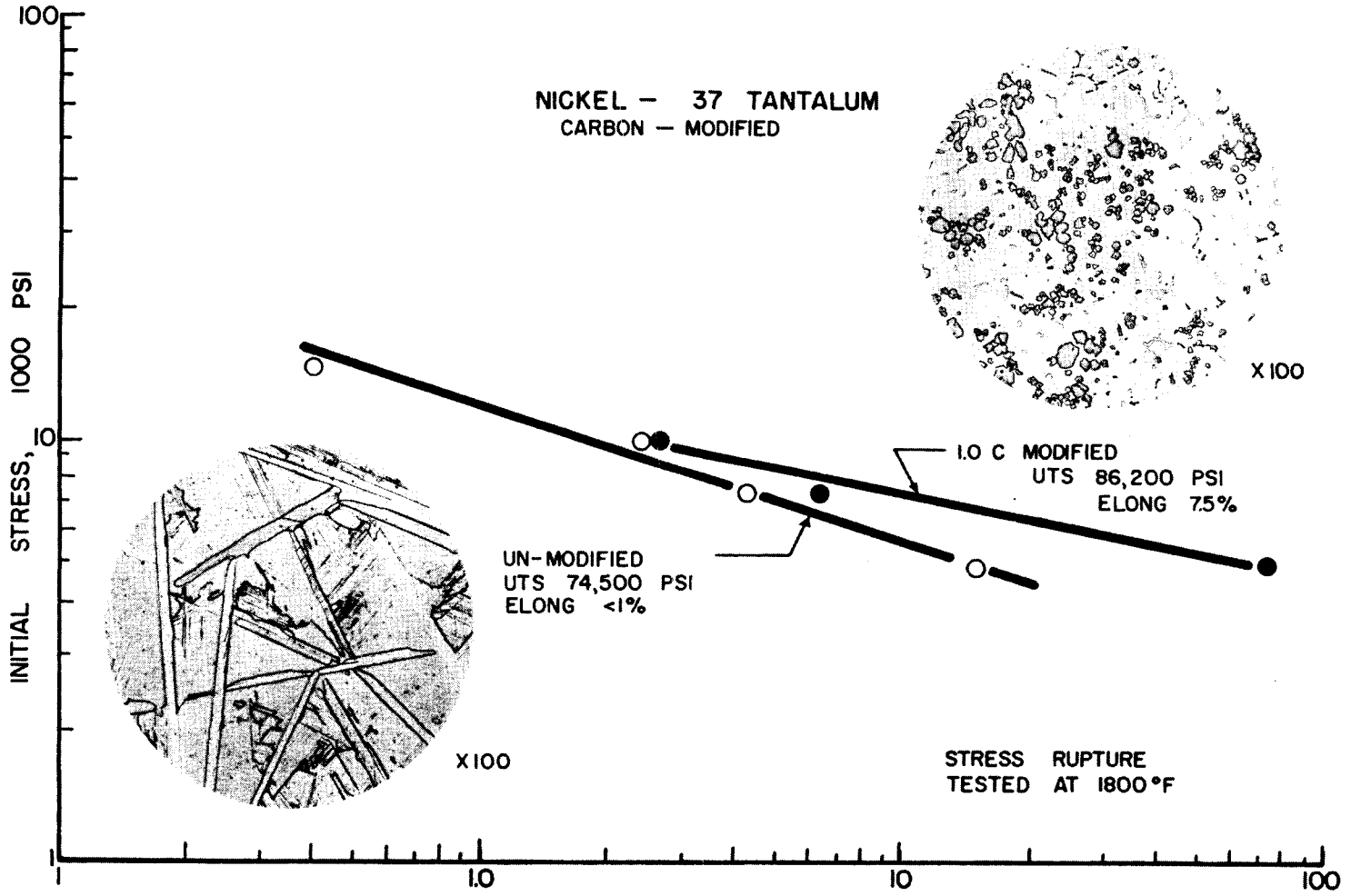

FIG. 22. EFFECT OF CARBON-MODIFICATION ON THE STRUCTURE AND PROPERTIES OF THE EUTECTIC ALLOY NICKEL – 37 TANTALUM.
REDUCED APPROXIMATELY 26 PERCENT IN PRINTING.

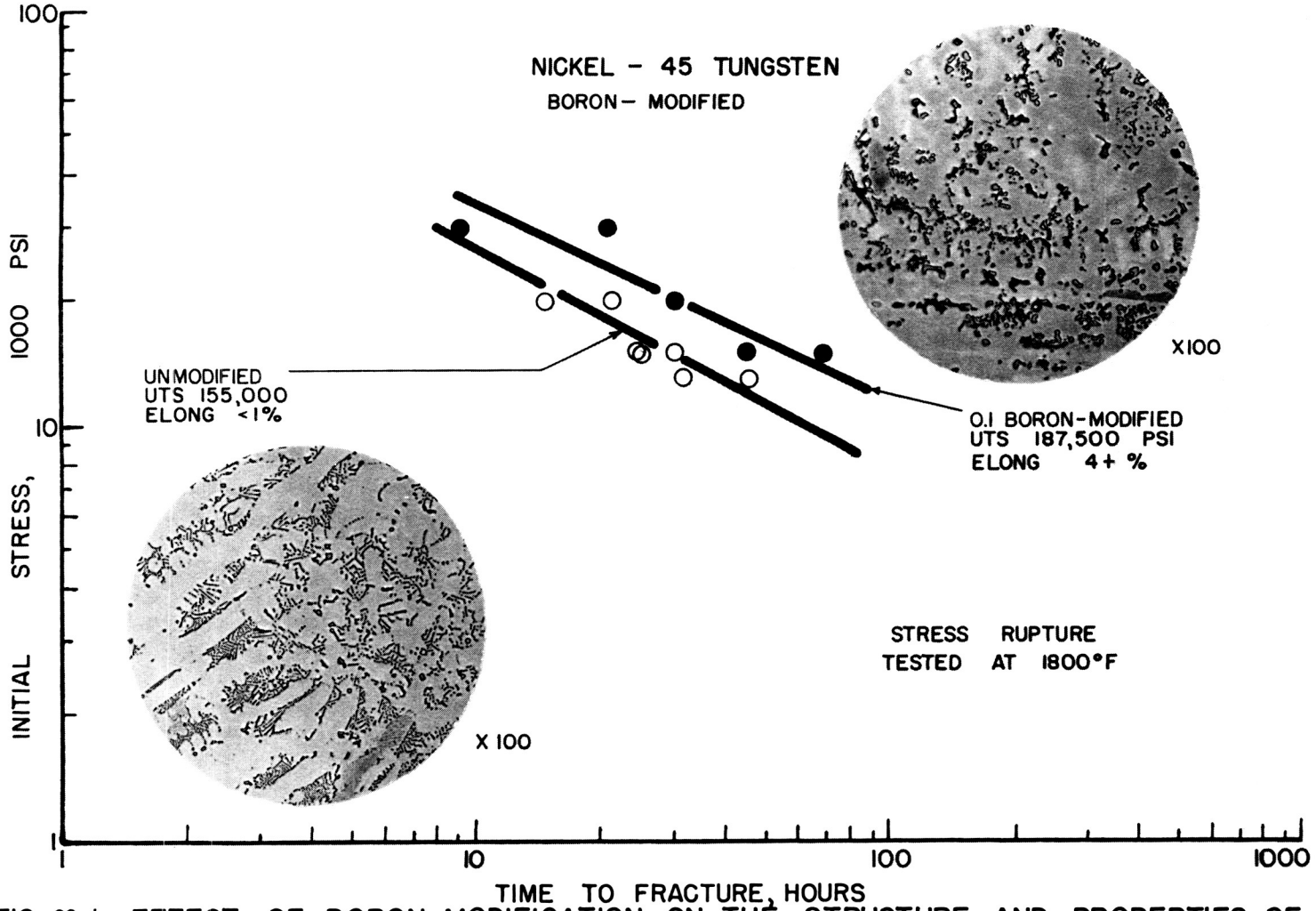

FIG. 23 : EFFECT OF BORON-MODIFICATION ON THE STRUCTURE AND PROPERTIES OF THE EUTECTIC ALLOY NICKEL-45 TUNGSTEN.
REDUCED APPROXIMATELY 26 PERCENT IN PRINTING.

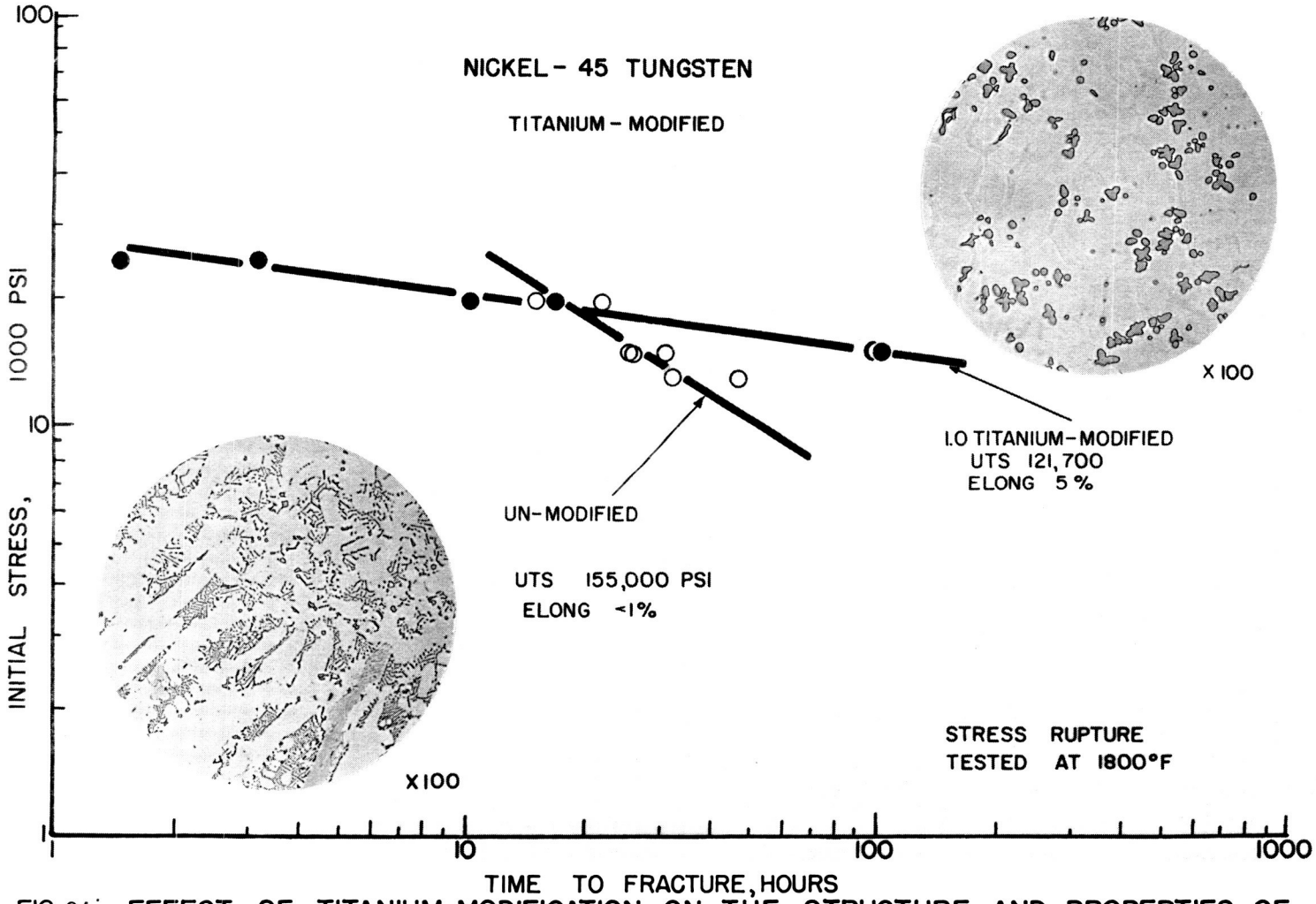

FIG. 24. EFFECT OF TITANIUM-MODIFICATION ON THE STRUCTURE AND PROPERTIES OF THE EUTECTIC ALLOY NICKEL-45 W.
REDUCED APPROXIMATELY 26 PERCENT IN PRINTING.

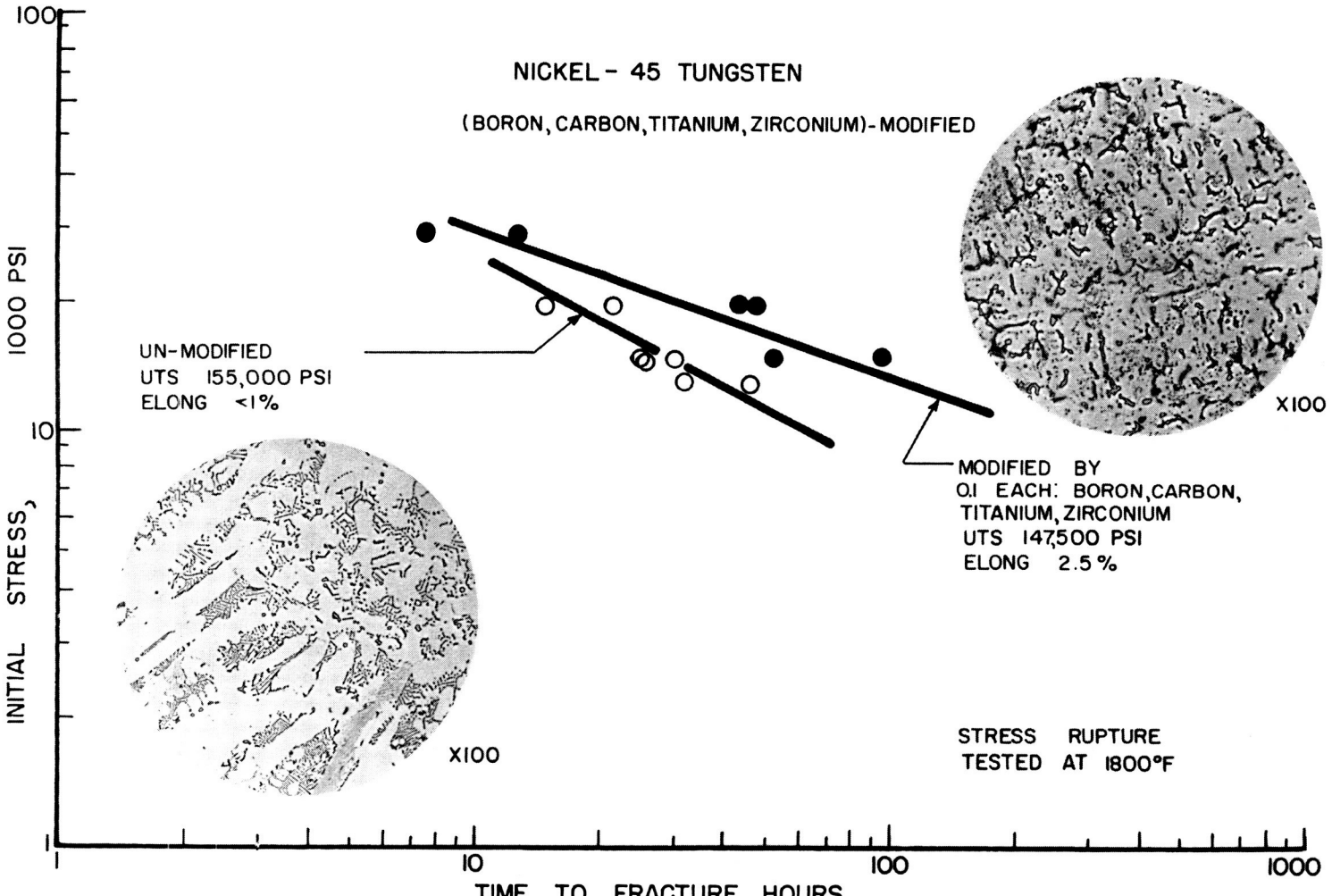

FIG. 25 :EFFECT OF (BORON, CARBON, TITANIUM, ZIRCONIUM) MODIFICATION ON THE STRUCTURE AND PROPERTIES OF THE EUTECTIC ALLOY NICKEL-45 TUNGSTEN.
REDUCED APPROXIMATELY 26 PERCENT IN PRINTING.

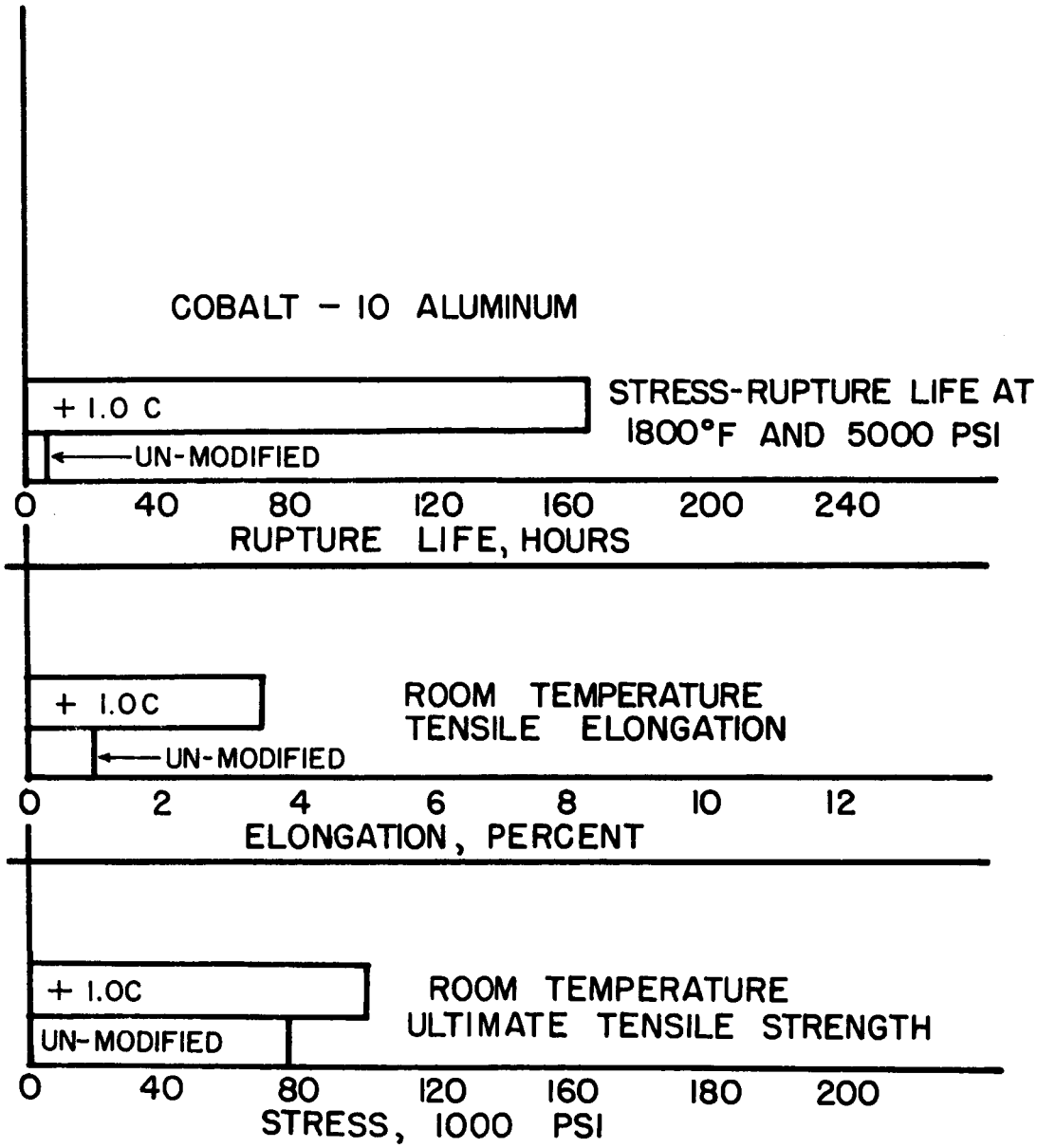

FIG. 26: EFFECT OF MODIFICATION ON THE ROOM TEMPERATURE TENSILE PROPERTIES AND STRESS RUPTURE LIFE AT 1800°F AND 5000 PSI OF THE EUTECTIC ALLOY COBALT - 10 ALUMINUM.

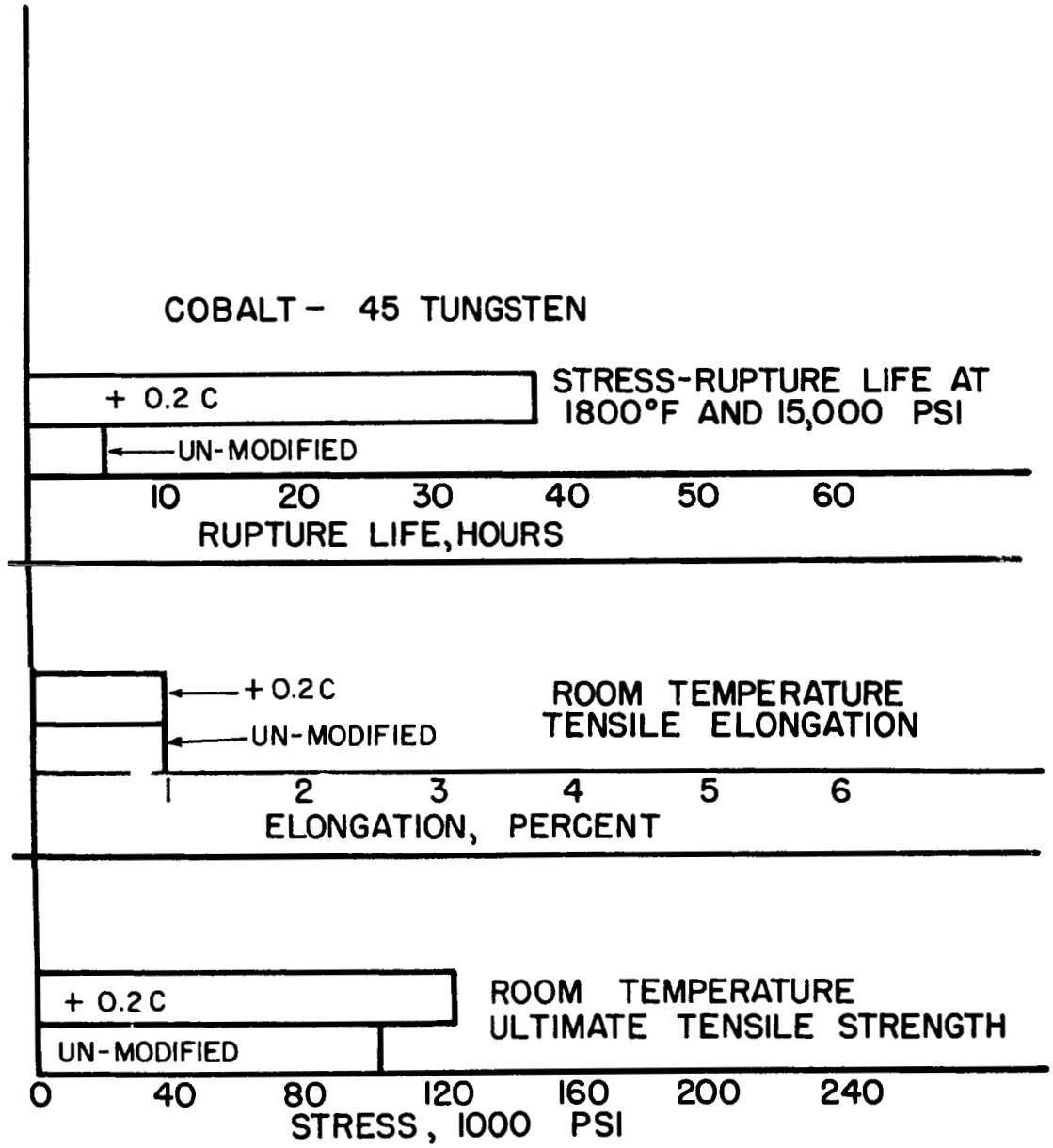

FIG. 27: EFFECT OF MODIFICATION ON THE ROOM TEMPERATURE TENSILE PROPERTIES AND STRESS RUPTURE LIFE AT 1800°F AND 15,000 PSI OF THE EUTECTIC ALLOY COBALT-45 TUNGSTEN.

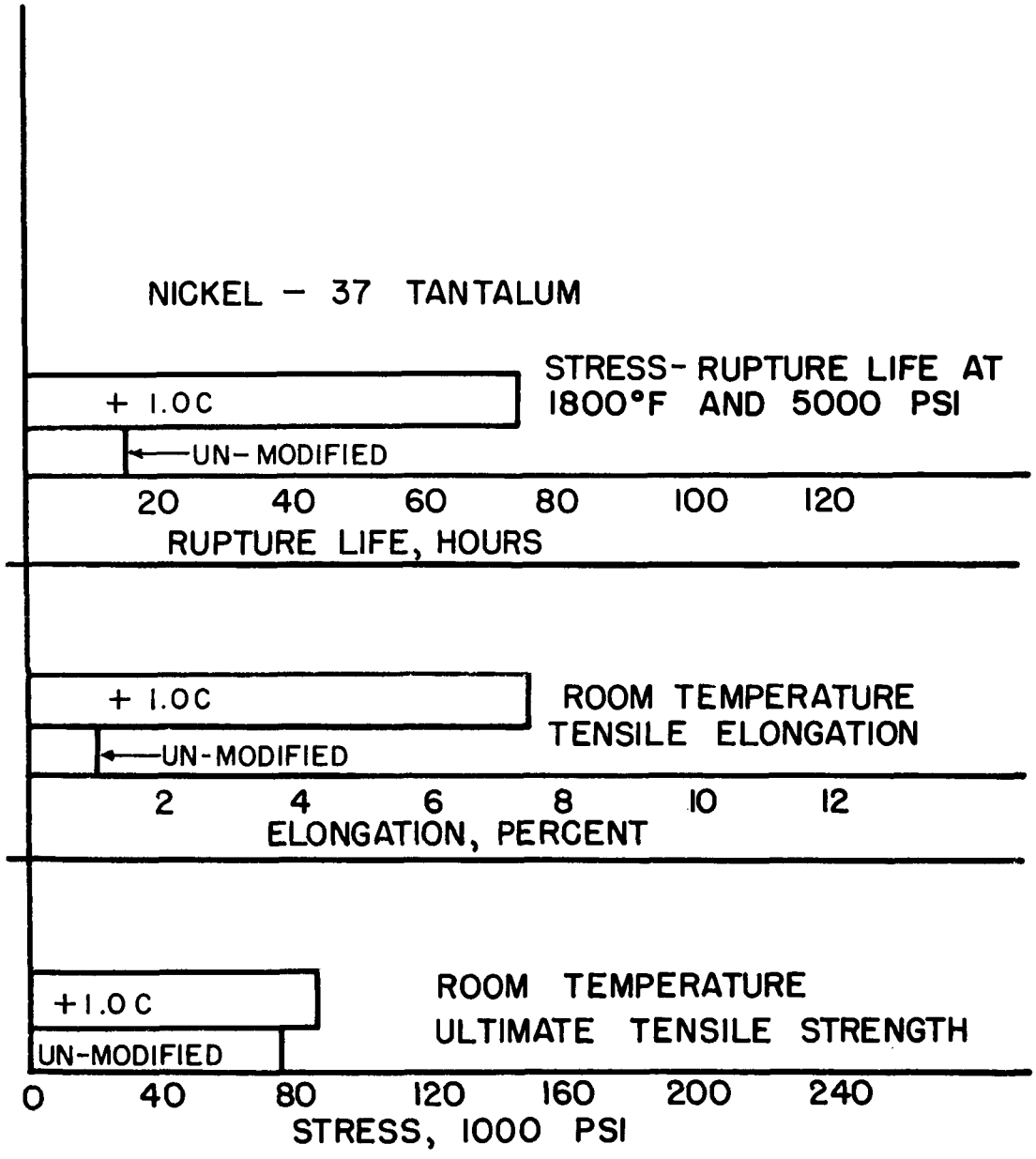

FIG. 28 : EFFECT OF MODIFICATION ON THE ROOM TEMPERATURE TENSILE PROPERTIES AND STRESS RUPTURE LIFE AT 1800°F AND 5000 PSI OF THE EUTECTIC ALLOY NICKEL-37 TANTALUM.

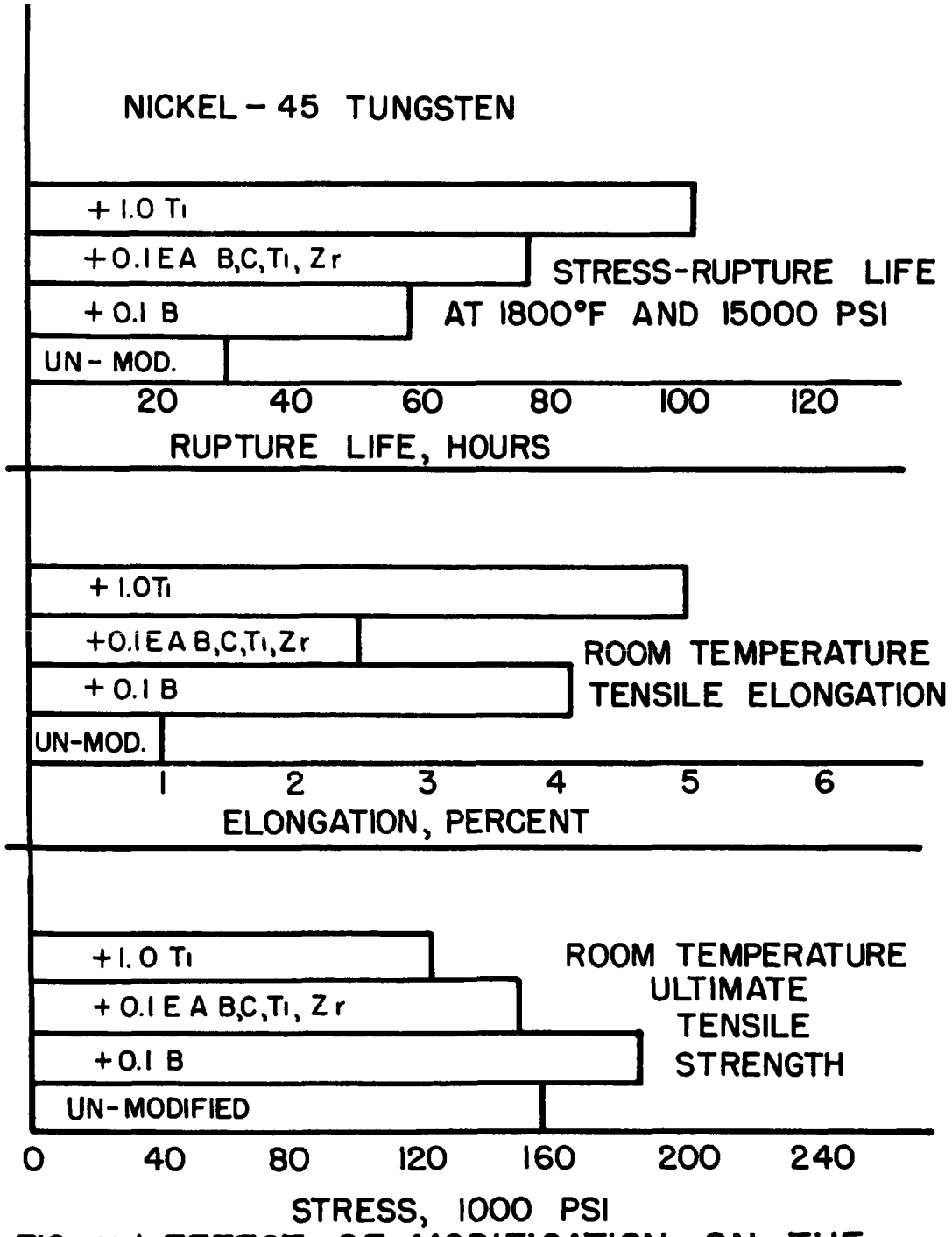

FIG. 29: EFFECT OF MODIFICATION ON THE ROOM TEMPERATURE TENSILE PROPERTIES AND STRESS RUPTURE LIFE AT 1800°F AND 15000 PSI OF THE EUTECTIC ALLOY NICKEL - 45 TUNGSTEN.

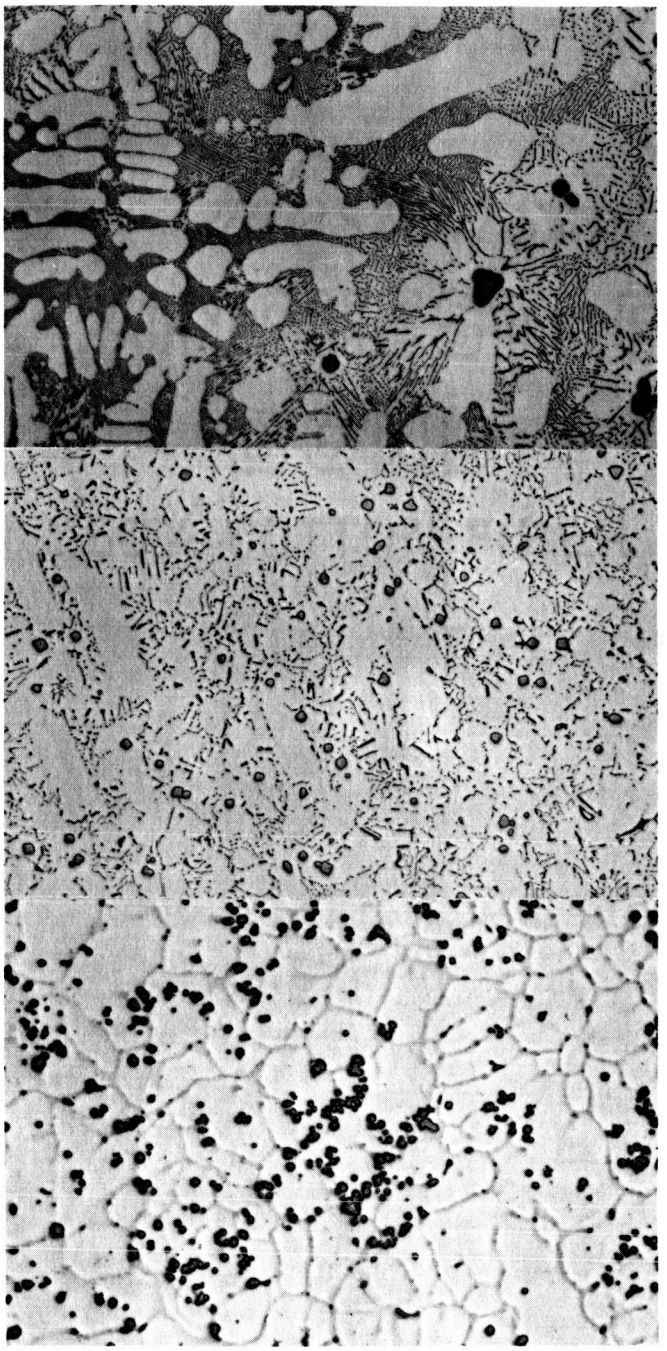

a)

Unmodified
X100

b)

+0.1 Titanium

X100

c)

+1.0 Titanium
X100

Figure 30. Effect of titanium on the formation of primary tungsten particles in Ni-45W.

ACKNOWLEDGMENTS

I should like to express my appreciation to the following:

1. To the National Aeronautics and Space Administration for its generous support of this work,
2. To Professor John F. Wallace for having stimulated my interest in and increased my understanding of solidification,
3. To many people at Lewis Research Center of NASA for their help and encouragement,
4. To Mr. W. H. Holt and Mr. R. G. Howe for their considerable help with the experimental work.

R. L. Ashbrook
Cleveland, Ohio
1965